

Self-assembled nickel cubanes as oxygen evolution catalysts

Ana Cristina García-Álvarez,^a Stefani Gamboa-Ramírez,^b Diego Martínez-Otero,^c Maylis Orio,^{*b} and Ivan Castillo^{*a}

^a Instituto de Química, Universidad Nacional Autónoma de México, Circuito Exterior, CU, Ciudad de México 04510, Mexico

^b Aix Marseille Université, CNRS, Centrale Marseille, iSm2, 13397, Marseille, France

^c Centro Conjunto de Investigación en Química Sustentable UAEM-UNAM, Carretera Toluca-Atlacomulco km. 14.5, Toluca, 50200, Estado de México, Mexico

Table of Contents

Experimental Procedures	S2
Synthesis and Characterization	S3
Synthesis and characterization of 1	S3
Synthesis and characterization of 2	S4
Synthesis and characterization of 3	S5
Electrochemical data.....	S8
Stability of 1 and 2	S15
Scanning Electrode Microscopy	S15
UV-Vis experiments	S16
Successive cyclic voltammogram scans of 1 and 2	S17
Mechanistic studies	S18
Electrochemical characterization of 3	S20
Dioxygen quantification	S23
DFT calculations	S26
References	S51

Experimental Procedures

Materials and methods

All chemicals are of the highest commercially available purity and were used as received, unless noted otherwise. Water used in all experiments was distilled and deionized by a Milli-Q system from Millipore. The ligand 1-methyl-2-benzimidazolemethanol (**L²**) was synthesized according to reported procedures.¹ Elemental analyses were obtained with a Thermo Scientific elemental analyzer Flash 2000, at a temperature of 950°C using an XP6 Mettler Toledo microbalance; methionine from Thermo Scientific with certification number 237031 was used as standard. UV-vis spectra were obtained with an Agilent 8453 spectrometer at room temperature. CV and controlled potential bulk electrolysis were performed on a CHI 1200B electrochemical workstation in buffered (pH7) phosphate aqueous solutions at room temperature using an Ag/AgCl reference electrode, a glassy carbon working electrode and a Pt auxiliary electrode; pH was measured using a pH electrode (HI9812) from Hanna Instruments. O₂ evolution was measured with a YSI 5100 Dissolved Oxygen Meter. ¹H NMR spectra were recorded on a Bruker Avance 300 MHz spectrometer. EPR spectra were obtained with a Jeol JES-TE300 equipment. The EPR spectral simulations were performed using Matlab program package Easyspin.² The optimum Hamiltonian parameters were obtained with an exact diagonalization. The homogenous linewidth was set to 0.6 mT to simulate the width of the recorded lines and A_N was considered isotropic. The Hamiltonian used for the simulations is the following: $H = \mu_b S[g]B + S[A_N]I_N + \text{nuclear Zeeman}$.

Crystallographic Data

Intensity data were collected on a Bruker Apex-Duo diffractometer. The structures were solved by direct methods (SHELXT). A crystal of **1** (0.081 × 0.046 × 0.028 mm in size) was mounted on a cryoloop with Paratone oil. Data were collected in a nitrogen gas stream at 100(2) K. Data collection was 97.5% complete. A total of 8745 reflections were collected covering the indices, -12<=h<=13, -17<=k<=17, 0<=l<=19. The total of reflections was found to be symmetry independent. Indexing and unit cell refinement indicated a primitive, triclinic lattice. For **2**, a crystal (0.118 × 0.112 × 0.033 mm in size) was mounted for data collection in a nitrogen gas stream at 100(2) K to 97.7% completeness. A total of 77979 reflections were collected covering the indices, -17<=h<=18, -18<=k<=18, -20<=l<=20. 13578 reflections were found to be symmetry independent, with R_{int} of 0.0730. Indexing and unit cell refinement indicated a primitive, triclinic lattice. See **Table S1**.

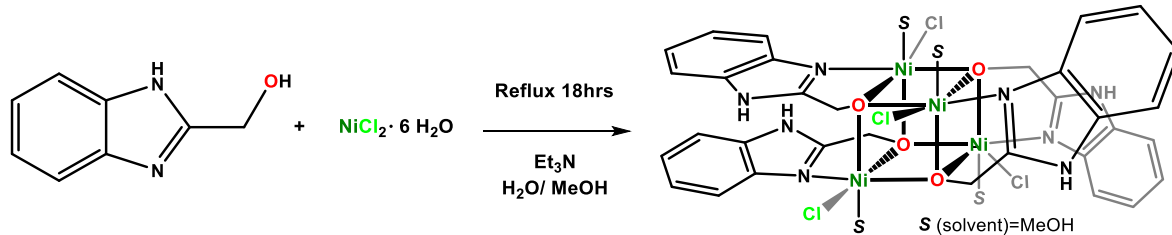
Computational parameters

All calculations were performed using the ORCA program package.³ Full geometry optimizations were carried out for all complexes in the high-spin state using the GGA functional BP86⁴⁻⁶ in combination with the def2-TZV/P⁷ basis set for all atoms and by taking advantage of the resolution of the identity (RI) approximation in the Split-RI-J variant⁸ with the appropriate Coulomb fitting sets.⁹ Increased integration grids (Grid4 in ORCA convention) and tight SCF convergence criteria were used. For according to the experimental conditions, these calculations were performed in gas phase and in water solvent by invoking the Control of the Conductor-like Polarizable Continuum Model (CPCM).¹⁰ To ensure that the resulting structures converged to a local minimum on the potential energy surface, frequency calculations were performed and resulted in only positive normal vibrations. The relative energies were computed from the gas-phase optimized structures as a sum of electronic energy, solvation and thermal corrections to the free energy. Electronic structures were obtained from single-point Broken-Symmetry DFT calculations using the hybrid functional B3LYP^{11,12} together with the def2-TZVP basis set. All possible spin configurations for the broken-symmetry¹³⁻¹⁵ calculations were generated with the "FlipSpin" feature of ORCA. Redox potentials are obtained from the calculated free energy change between oxidized and reduced species in solution. They are relative potentials referenced to standard hydrogen electrode and as such, a value of 4.28 eV was subtracted to make direct comparisons to experimental data.^{16,17} EPR parameters including g-tensors and hyperfine coupling constants were obtained from additional single-point calculations using the B3LYP functional. The triply polarized core property basis set CP(PPP)¹⁸ was applied for the metal centers, while the EPR-II¹⁹ basis set was used for all remaining atoms.

Optical properties were predicted from additional single-point calculations using the def2-TZV/P basis in combination with the hybrid GGA functional PBE0.²⁰ Vertical electronic transitions were calculated using simplified time-dependent DFT within the Tamm–Dancoff approximation (sTDA).^{21,22} To increase computational efficiency, the RI approximation²³ was used in calculating the Coulomb term, and at least 30 excited states were calculated in each case. Spin density plots as well as molecular orbitals were generated using the orca plot utility program and were visualized with the Chemcraft program.²⁴ All the results presented in this reported are obtained from calculations conducted in water.

Synthesis and Characterization

Synthesis and characterization of 1



Scheme S1. Synthesis of 1.

For the synthesis of **1**, 2-benzimidazolmethanol (**L**¹, 0.30 g, 2.02 mmol) and $\text{NiCl}_2 \cdot 6\text{H}_2\text{O}$ (0.48 g, 2.02 mmol) were stirred at reflux temperature for 18 hours in a 1:1 water/methanol mixture in the presence of triethylamine (0.42 ml, 3.04 mmol). The light green solution was filtered over celite and then evaporated to dryness, and finally washed with diethyl ether (3x2 mL). M.p. 94–95°C. Yield 85%. FAB⁺ MS m/z 846 [$\text{Ni}_4\text{L}_4^{14}\text{Cl}_3^+$] (**Figure S1**). ESI-MS m/z 928.6 [$\text{Ni}_4\text{L}_4\text{Cl}_3^+$] (**Figure S2**). Combustion Analysis Calc. for $\text{C}_{36}\text{H}_{40}\text{Cl}_4\text{N}_8\text{Ni}_4\text{O}_8$: C, 39.66; H, 3.70; N, 10.29%. Found C, 39.66; H, 3.51; N, 10.21%. IR(KBr) 3057 cm⁻¹(Ar-H); 2977 cm⁻¹(C-H); 2924 cm⁻¹(C-H); 1570 cm⁻¹(C=N); 1454 cm⁻¹(C-H); 1396 cm⁻¹(C-H); 1277 cm⁻¹(N-H in-plane-bending); 837 cm⁻¹(N-H out-of-plane-bending). UV-vis (MeOH): 211 nm ($\epsilon = 17,180 \text{ M}^{-1}\text{cm}^{-1}$), 243 (6,370), 273 (8,940), 281 (9,160), 296 (1,580), 340 (430), 670 (24).

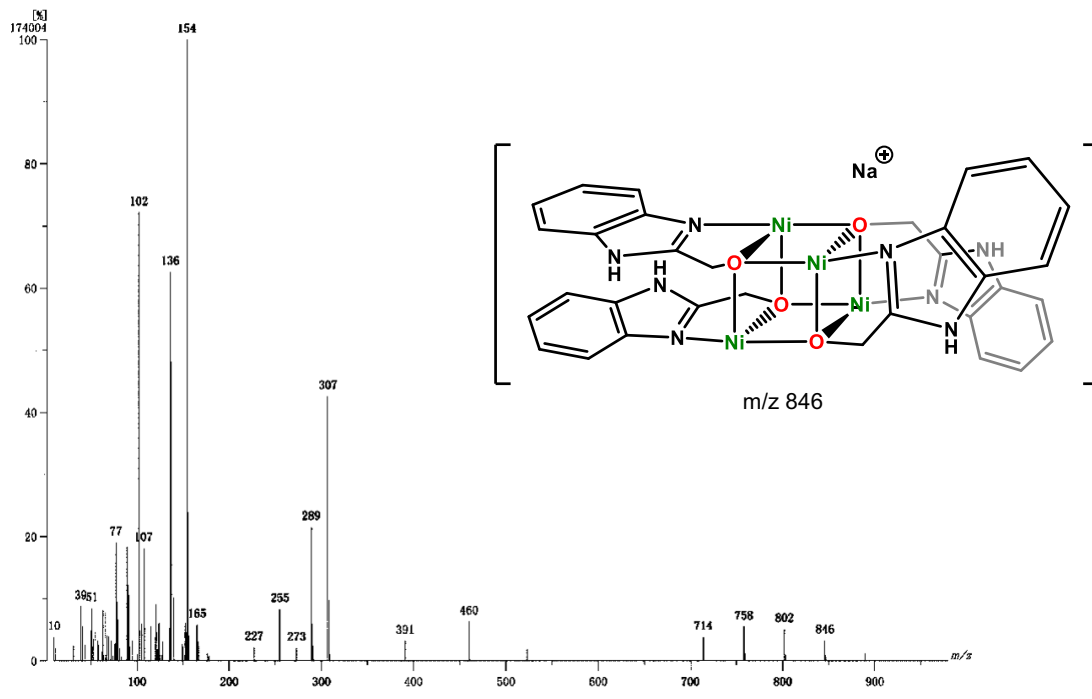


Figure S1. a) FAB⁺ MS of **1**.²⁵

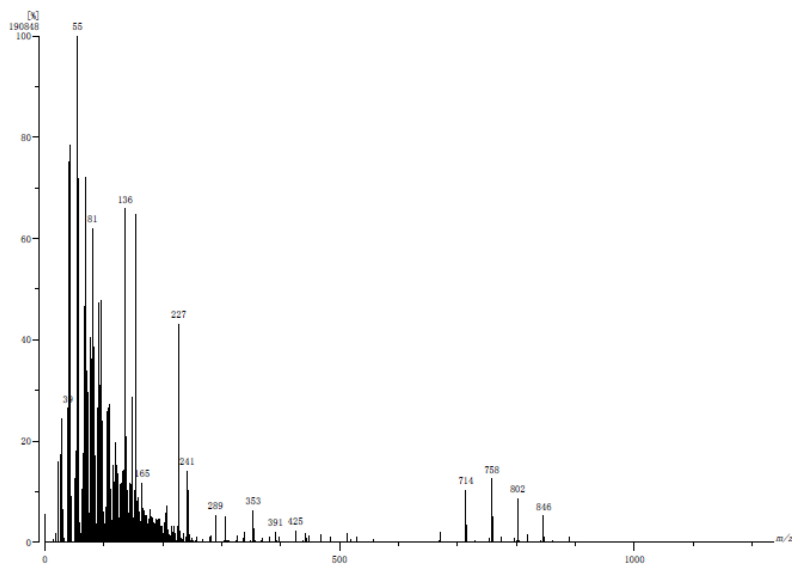


Figure S1. b) FAB⁺ MS of **1** after electrolysis.

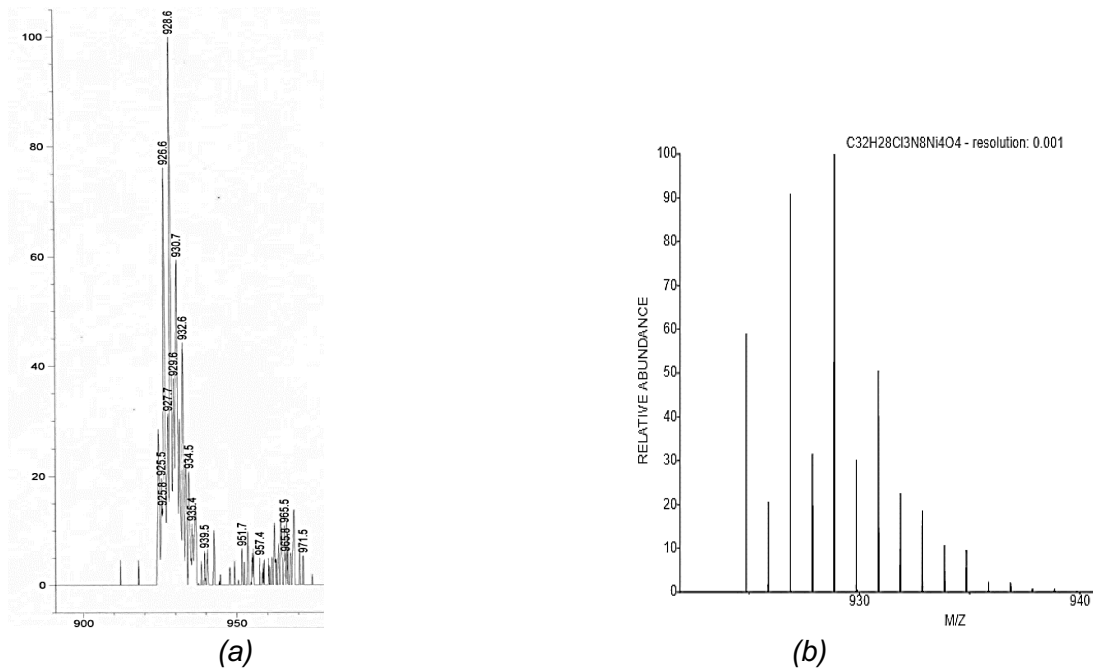


Figure S2. (a) ESI MS of **1** at m/z 928.6 assigned to $[Ni_4L^4Cl_3]^+$ and (b) calculated isotopic pattern.

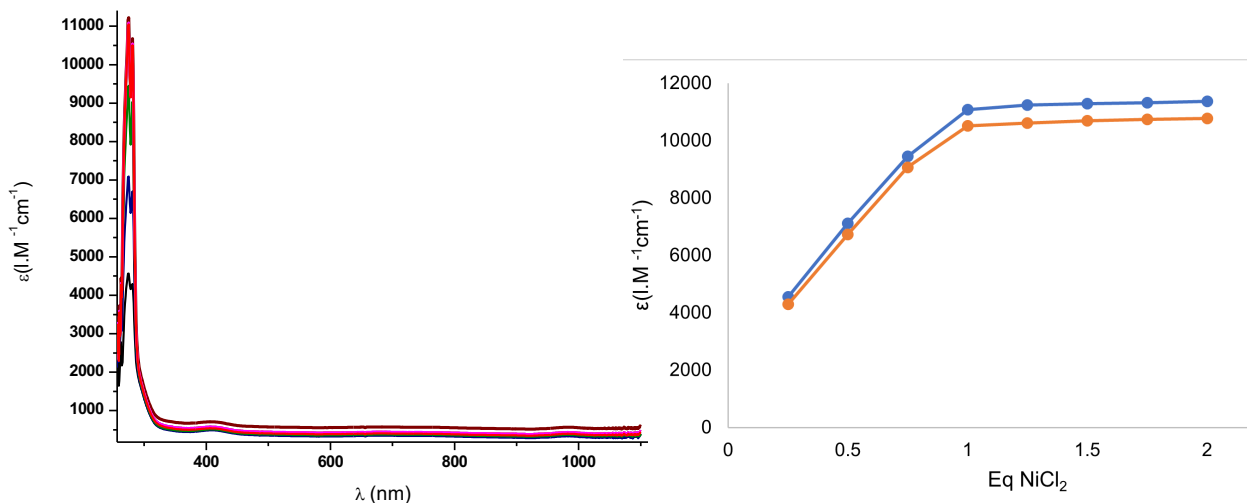
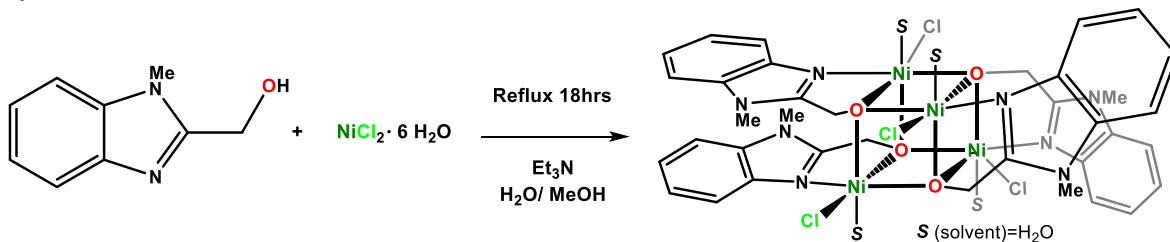


Figure S2. (c) Left: UV-vis spectra of the titration of NiCl_2 (0.25- 2.0 equivalents) with $\text{L}^1\text{OH}/\text{NEt}_3$ in DMF; right: absorbance plot at 274 (blue trace) and 281 nm (orange trace) vs number of equivalents of NiCl_2 .

Synthesis and characterization of **2**



Scheme S2. Synthesis of **2**.

For the synthesis of **2**, 1-methyl-2-benzimidazolemethanol (L^2 , 0.30 g, 1.85 mmol) and $\text{NiCl}_2 \cdot 6\text{H}_2\text{O}$ (0.44 g, 1.85 mmol) were heated to reflux for 18 hours in a 1:1 water/methanol mixture in the presence of triethylamine (0.42 mL, 3.04 mmol). The light green solution was filtered through celite and evaporated to dryness, finally the solid obtained was washed with diethyl ether (3 x 2 mL). M.p. 187-188°C. Yield 63%. FAB⁺ MS m/z 986 $[\text{Ni}_4\text{L}^2_4\text{Cl}_3]^+$ (**Figure S3**). Combustion Analysis Calc. for $\text{C}_{36}\text{H}_{44}\text{Cl}_4\text{N}_8\text{Ni}_4\text{O}_8$ C, 38.91; H, 4.17; N, 9.88%. Found C, 38.89; H, 4.11; N, 9.44%. IR(KBr) 2919 cm^{-1} (HC-H); 2849 cm^{-1} (H₂C-H); 1614 cm^{-1} (C=N); 742 cm^{-1} (Ar-R₂). UV-vis (MeOH): 208 nm ($\epsilon = 20,420 \text{ M}^{-1}\text{cm}^{-1}$), 275 (17,800), 418 (63), 680 (30).

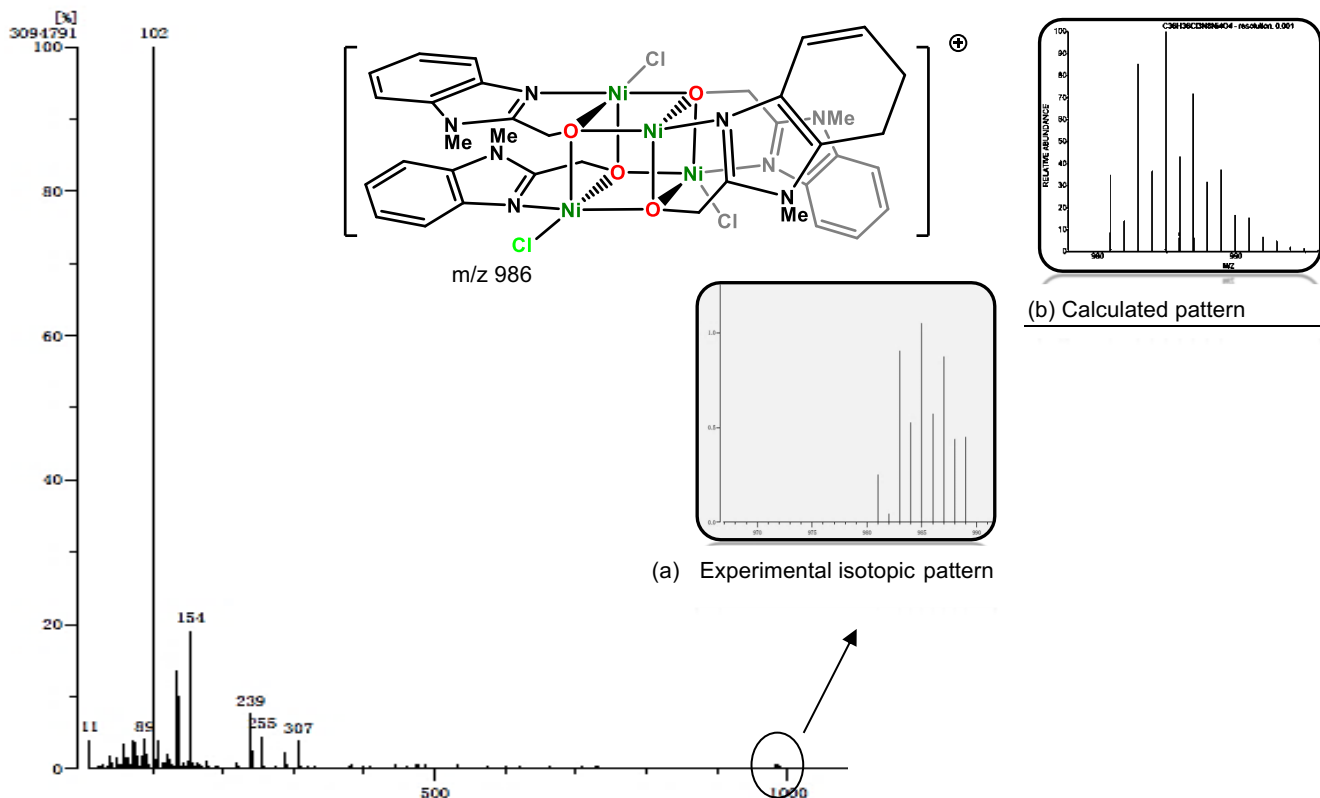
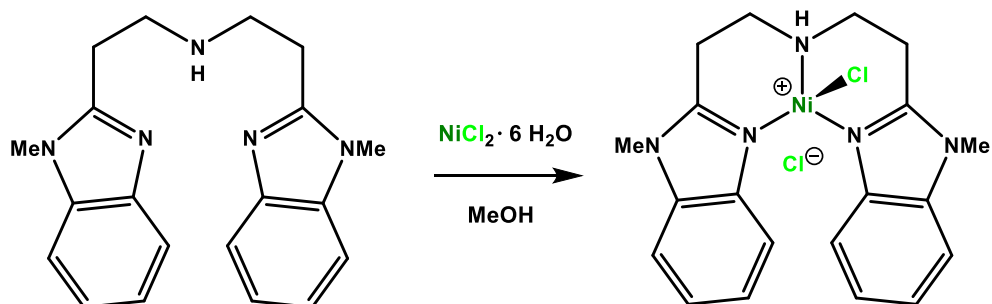


Figure S3. FAB⁺ MS of **2** with (a) experimental isotopic pattern at *m/z* 986 assigned to $[Ni_4L^2_4Cl_3]^+$, and (b) calculated isotopic pattern.

Synthesis and characterization of **3**



Scheme S3. Synthesis of **3**.

For the synthesis of **3**, bis(2-(1-methyl-1H-benzimidazol-2-yl)ethyl)amine (L^3 , 0.30 g, 0.90 mmol) and $NiCl_2 \cdot 6H_2O$ (0.21 g, 0.90 mmol) were stirred for 18 hours in methanol at room temperature. The green solution was filtered through celite and evaporated to dryness, finally the solid obtained was washed with diethyl ether (3×2 mL). The compound decomposes above 310°C. Yield 82%. FAB⁺ MS *m/z* 391 $[NiL^3]^+$. ESI MS *m/z* 426 $[NiL^3Cl]^+$ (**Figure S4**). Combustion Analysis Calc. for $C_{21}H_{28}Cl_2N_5NiO_2$ C, 49.26; H, 5.51; N, 13.68%. Found C, 48.92; H, 5.13; N, 14.04%. IR(KBr) 3471 (H-OCH₃, H-O-H); 3139 (Ar-C-H); 2950, 2900, 2869 (H-CH₂, -HCH); 1614 (C=N); 1487, 1457, 1412 (Ar-C=C, -CH₃); 767, 759 (H-CH₂, -HCH) cm⁻¹. UV-vis (MeOH): 213 nm ($\epsilon = 21,300 M^{-1}cm^{-1}$), 253 (14,040), 274 (16,990), 388 (60), 635 (13).

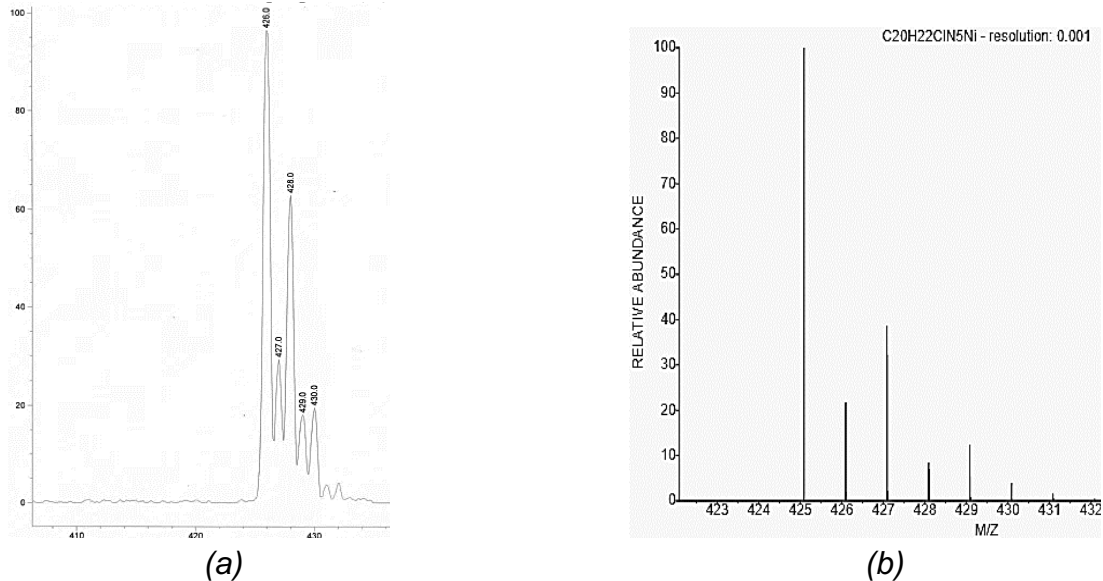


Figure S4. (a) ESI MS of **3**, m/z 426 assigned as $[\text{NiL}^3\text{Cl}]^+$, (b) calculated isotopic pattern.

Table S1. Crystal data and structure refinement of **1** and **2**

Complex	1	2
Empirical formula	C38 H52 Cl4 N8 Ni4 O10	C47 H55.74 Cl26 N8 Ni4 O8.37
Formula weight	1157.51	2023.19
Temperature	100(2) K	100(2) K
Wavelength	1.54178 Å	1.54178 Å
Crystal system	Triclinic	Triclinic
Space group	$P\bar{1}$	$P\bar{1}$
Unit cell dimensions	$a = 10.8544(10)$ Å $\alpha = 86.3726(7)^\circ$ $b = 13.9030(2)$ Å $\beta = 72.2389(8)^\circ$ $c = 16.2102(2)$ Å $\gamma = 86.3793(7)^\circ$	$a = 15.1023(6)$ Å $\alpha = 93.357(3)^\circ$ $b = 15.5842(6)$ Å $\beta = 108.671(2)^\circ$ $c = 17.1586(7)$ Å $\gamma = 94.518(3)^\circ$
Volume	2322.52(5) Å ³	3798.9(3) Å ³
Z	2	2
Density (calculated)	1.655 Mg/m ³	1.769 Mg/m ³
Absorption coefficient	4.467 mm ⁻¹	9.975 mm ⁻¹
F(000)	1192	2029
Crystal size	0.081 × 0.046 × 0.028 mm ³	0.118 × 0.112 × 0.033 mm ³
Θ range data collection	2.865 to 71.816°	2.729 to 68.245°
Index ranges	-12≤h≤13, -17≤k≤17, 0≤l≤19	-17≤h≤18, -18≤k≤18, -20≤l≤20
Reflections collected	8745	77979
Completeness Θ=67.679°	97.5 %	97.7 %
Refinement method	Full-matrix least-squares on F^2	Full-matrix least-squares on F^2
Data/restraints/param.	8745 / 612 / 740	13578 / 3296 / 1609
Goodness-of-fit on F^2	1.043	1.047
R indices [$I > 2\sigma(I)$]	R1 = 0.0341, wR2 = 0.0812	R1 = 0.0846, wR2 = 0.2322
R indices (all data)	R1 = 0.0442, wR2 = 0.0866	R1 = 0.1009, wR2 = 0.2500
Largest diff. peak and hole	0.425 and -0.464 e Å ⁻³	1.590 and -1.645 e Å ⁻³

Table S2. Hydrogen bonds in **1**

D-H...A	d(D-H)	d(H...A)	d(D...A)	\angle (DHA)
O(5)-H(5O)...Cl(2)	0.836(10)	2.282(14)	3.092(18)	163(3)
O(6)-H(6O)...Cl(4)	0.836(10)	2.202(14)	3.020(2)	166(4)
O(7)-H(7O)...Cl(1)	0.830(10)	2.265(14)	3.070(19)	163(3)
O(8)-H(8O)...Cl(3)	0.837(10)	2.175(11)	3.006(2)	172(3)
N(2)-H(2N)...O(9)	0.848(10)	1.941(11)	2.783(3)	172(3)
N(6)-H(6N)...Cl(1)1	0.858(7)	2.411(10)	3.250(2)	166(3)
N(8)-H(8N)...Cl(1)2	0.830(3)	2.440(3)	3.234(2)	162(3)

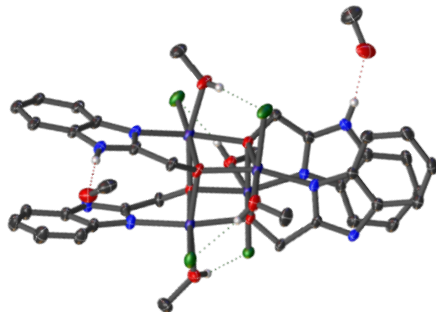


Figure S5. ORTEP diagram of **1**. Ellipsoids at 50% probability level, solvents molecules and H atoms (except those involved in H-bonding) are omitted for clarity. Cl···H and O···H interactions, both intramolecular and with solvent, are shown as dotted lines. See **Table S2**.

Table S3. Hydrogen bonds in **2**

D-H...A	d(D-H)	d(H...A)	d(D...A)	\angle (DHA)
O(5)-H(5B)...Cl(3)	0.839(10)	2.249(13)	3.070(5)	166(5)
O(5)-H(5C)...Cl(12)1	0.838(10)	2.960(7)	3.434(7)	118(6)
O(5)-H(5C)...Cl(15)1	0.838(10)	2.550(4)	3.235(7)	140(6)
O(5)-H(5C)...Cl(55)1	0.838(10)	2.668(15)	3.503(8)	174(6)
O(6)-H(6B)...Cl(4)	0.838(10)	2.255(13)	3.083(4)	168(5)
O(6)-H(6C)...Cl(4)2	0.842(10)	2.410(2)	3.192(4)	156(4)
O(7)-H(7A)...Cl(1)	0.840(10)	2.259(14)	3.019(5)	150(2)
O(7)-H(7B)...Cl(20)2	0.830(10)	2.910(3)	3.375(6)	118(2)
O(7)-H(7B)...Cl(79)2	0.830(10)	2.750(4)	3.430(2)	140(3)
O(8)-H(8E)...Cl(2)	0.840(5)	2.200(9)	3.017(4)	164(3)
O(8)-H(8F)...Cl(3)1	0.840(5)	2.500(2)	3.246(5)	148(3)

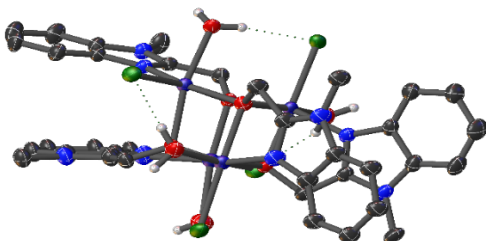


Figure S6. ORTEP diagram of **2**. Ellipsoids at 50% probability level, solvents molecules and H atoms (except those involved in H-bonding) are omitted for clarity. Intramolecular Cl···H interactions are shown as dotted lines. See **Table S3**.

Electrochemical data

Electrochemical data for 1

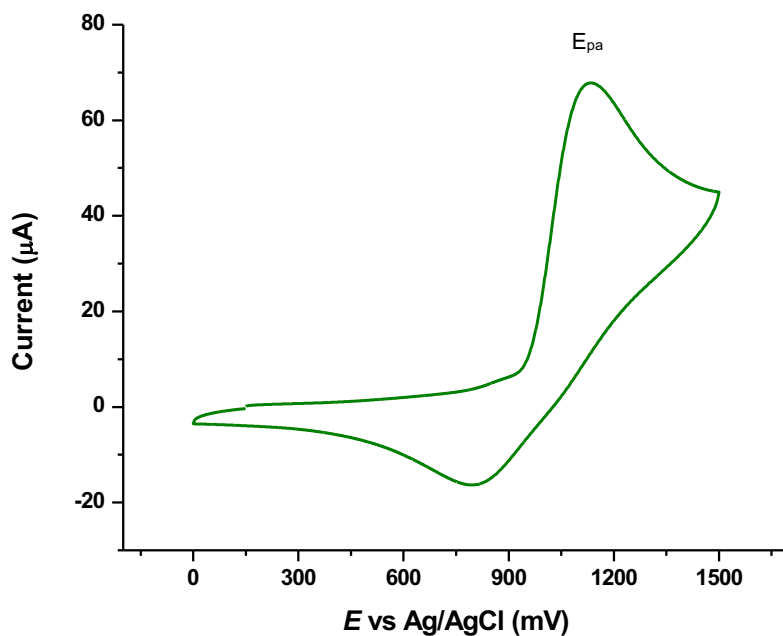


Figure S7. Cyclic voltammetry (CV) of **1** 0.15mM in DMF with 0.1 M tetrabutylammonium hexafluorophosphate (NBu_4PF_6) as electrolyte.

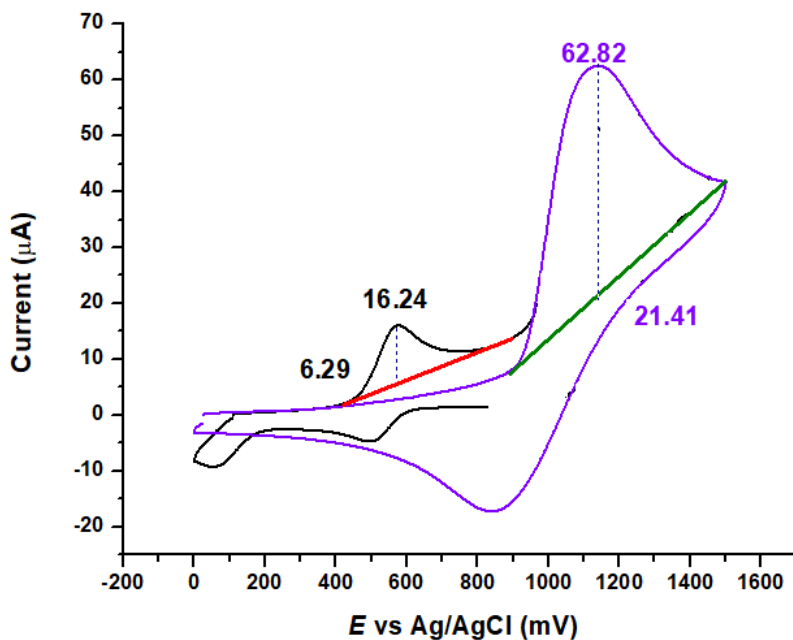


Figure S8. CV of 0.15 mM **1** (purple trace), and in the presence of ferrocene (black trace) in DMF with 0.1 mM NBu_4PF_6 .

- (a) CV of ferrocene (black)
Ferrocene $16.24 \mu\text{A} - 6.29 \mu\text{A} = 9.95 \mu\text{A}$
- (b) CV of **1** (violet)

$$62.82 \mu\text{A} - 21.41 \mu\text{A} = 41.41 \mu\text{A}$$

∴ Ratio between ferrocene in (a) and **1** in (b)

$$41.41 / 9.95 = 4.1$$

Approximation to diffusion coefficient of **1**

From Cottrell equation and chronoamperometry data analysis of **1**.

$$i = \frac{nFAC_0\sqrt{D}}{\sqrt{\pi t}}$$

where,

i = current

n = number of electrons (considering a 4 electron process)

F = Faraday constant

A = area of the electrode in cm²

C₀ = concentration

D = diffusion coefficient

t = time

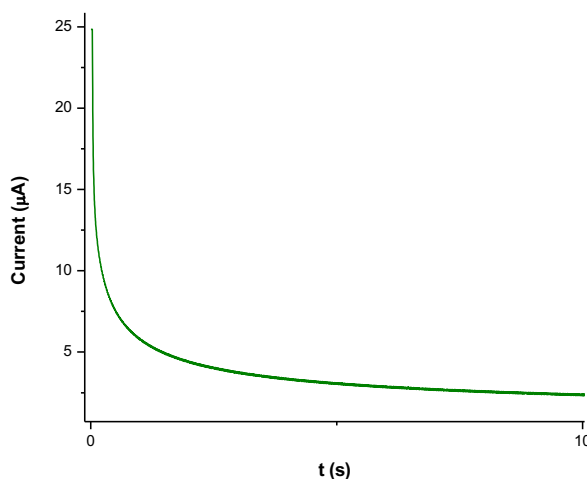


Figure S9. Chronoamperometry experiment of **1** 0.15mM in DMF with 0.1M NBu₄PF₆.

$$\therefore D_{\mathbf{1}}(\text{DMF}) \approx 1.1 \times 10^{-7} \text{ cm}^2 \text{s}^{-1}$$

Ferrocene diffusion coefficient reported.²⁶

$$D_{\text{Fc}}(\text{DMF}) \approx 1 \times 10^{-5} \text{ cm}^2 \text{s}^{-1}$$

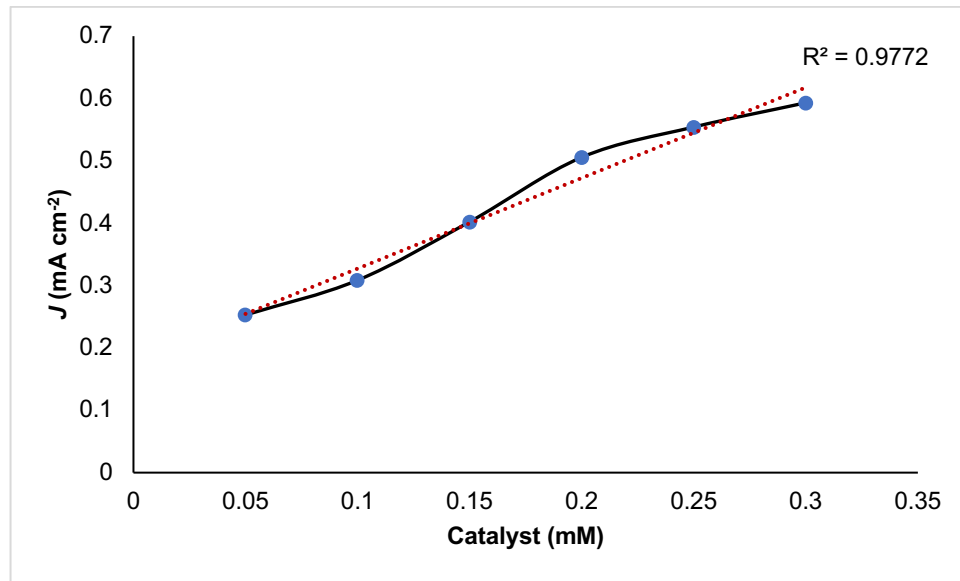


Figure S10. Catalytic current at 1.9 V as a function of the catalyst concentration from 0.05 to 0.35 mM measured in 0.1 M K-Pi buffer pH 7. Red line represents the best linear fit up to [1].

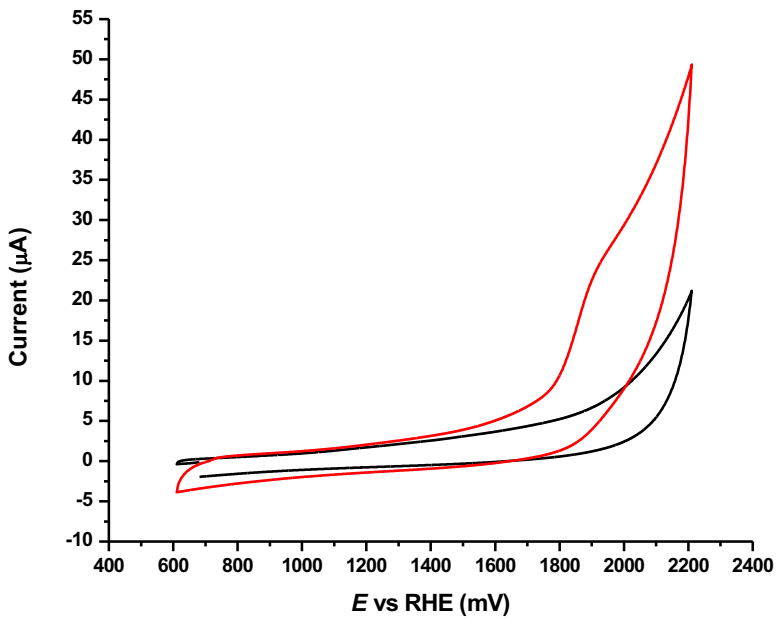


Figure S11. CV of 0.1 M potassium phosphate buffer (K-Pi) pH 7 (black) and 0.15 mM **1** in H₂O K-Pi (red). Scan rate = 100 mV s $^{-1}$, potential vs RHE.

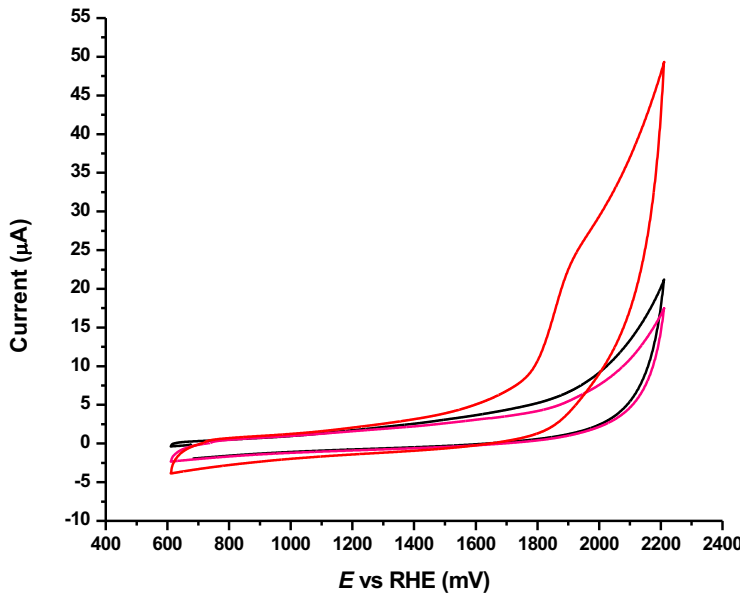


Figure S12. CV of 0.1 M K-Pi buffer pH 7 (black), 0.15 mM **1** in H_2O K-Pi (red). When the working electrode was removed from the catalyst-containing solution without washing and used in a clean buffer solution, no catalytic current was observed (pink). Scan rate = 100 mV s⁻¹.

Overpotential calculation for **1**^{27,28}

Overpotential calculation was carried out at pH 7 vs RHE.

$$E \text{ (vs. RHE)} = E_{\text{Ag}/\text{AgCl}} + 0.059 \text{ pH} + E^{\circ}_{\text{Ag}/\text{AgCl}}$$

$$E \text{ (vs. RHE)} = 1.15 + 0.413 + 0.198$$

$$E \text{ (vs. RHE)} = 1.76$$

$$\eta = E \text{ (vs. RHE)} - E^{\circ} \text{ (vs. RHE)} = 1.76 - 0.81 = 0.95 \text{ V} = 950 \text{ mV}$$

Overpotential calculation vs NHE

$$E_{\text{Ag}/\text{AgCl}} = 1.15 \text{ V}$$

$$\eta = E \text{ (vs. NHE)} - E^{\circ} \text{ (vs. NHE)} = 1.44 - 1.23 = 0.21 = 210 \text{ mV}$$

Rate constant calculation for **1**^{29a-c}

Data from **Figure S11**, at 100 mV s⁻¹

$$i_d / i_p = 1.38(k_{\text{obs}}/v)^{1/2}$$

$$6.25 = 1.38(k_{\text{obs}}/v)^{1/2}$$

$$\therefore k_{\text{obs}} = 2.05 \text{ s}^{-1}$$

The pseudo-first-order rate constant of the catalytic water oxidation, k_{cat} , is usually referred as turnover frequency (TOF) of the catalyst.³⁰

Electrochemical data for 2

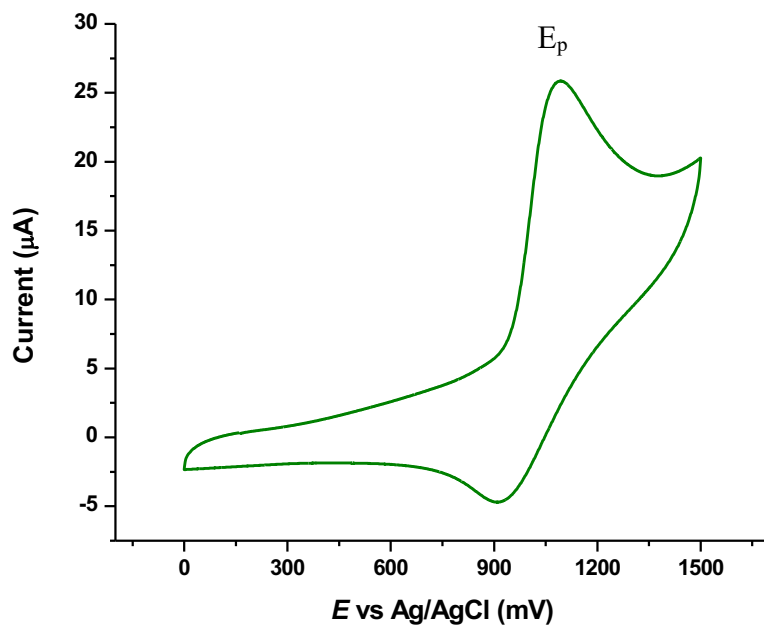


Figure S13. CV of **2** in DMF 0.1 mM NBu₄PF₆.

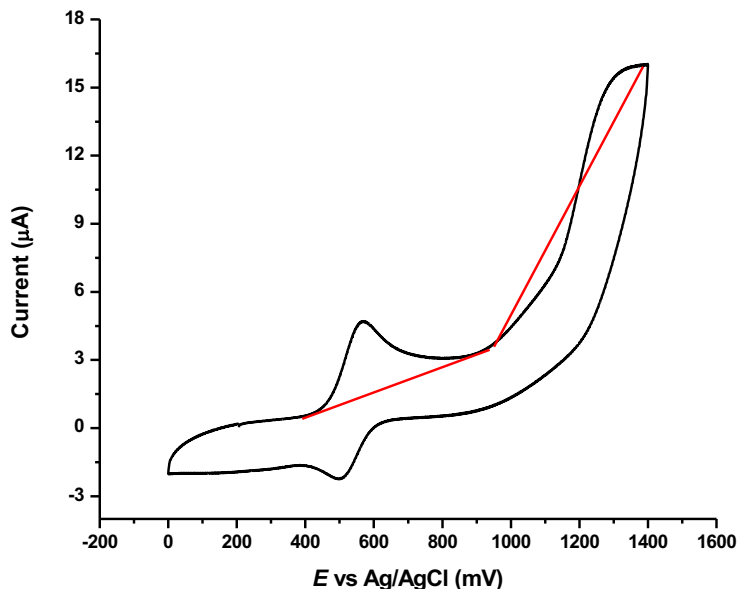


Figure S14. CV of 0.16 mM **2** in the presence of ferrocene (black trace) in DMF 0.1mM NBu₄PF₆.
(a) CV of ferrocene and **2** (black)

Ferrocene $3.33 \mu\text{A} - 0.55 \mu\text{A} = 2.78 \mu\text{A}$

$11.93 \mu\text{A} - 1.84 \mu\text{A} = 10.09 \mu\text{A}$

Ratio between ferrocene and **2** in (a)

$10.09/2.78 = 3.6$

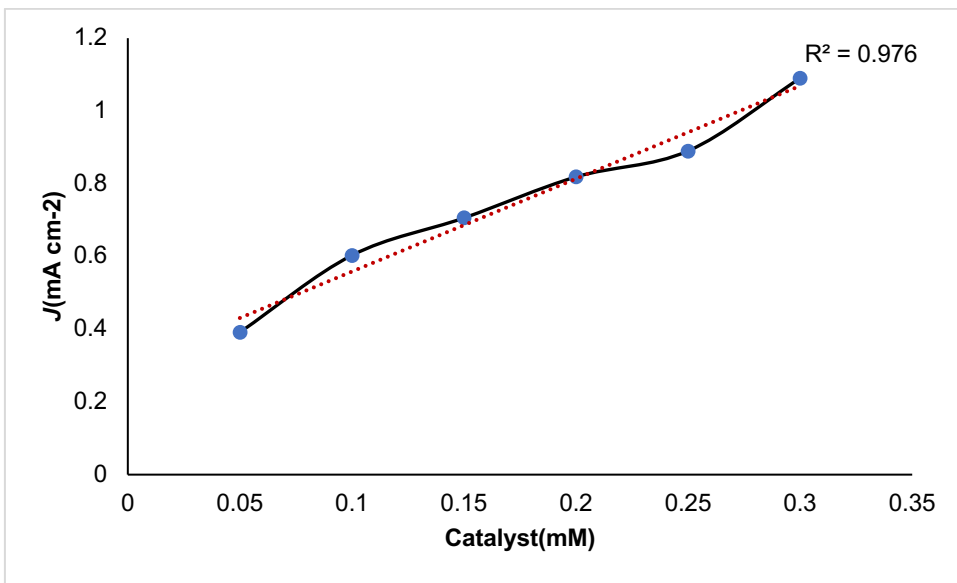


Figure S15. Catalytic current as a function of the catalyst concentration from 0.05 to 0.30 mM measured in 0.1 M K-Pi buffer pH 7. Red line represents the best linear fit up to [2].

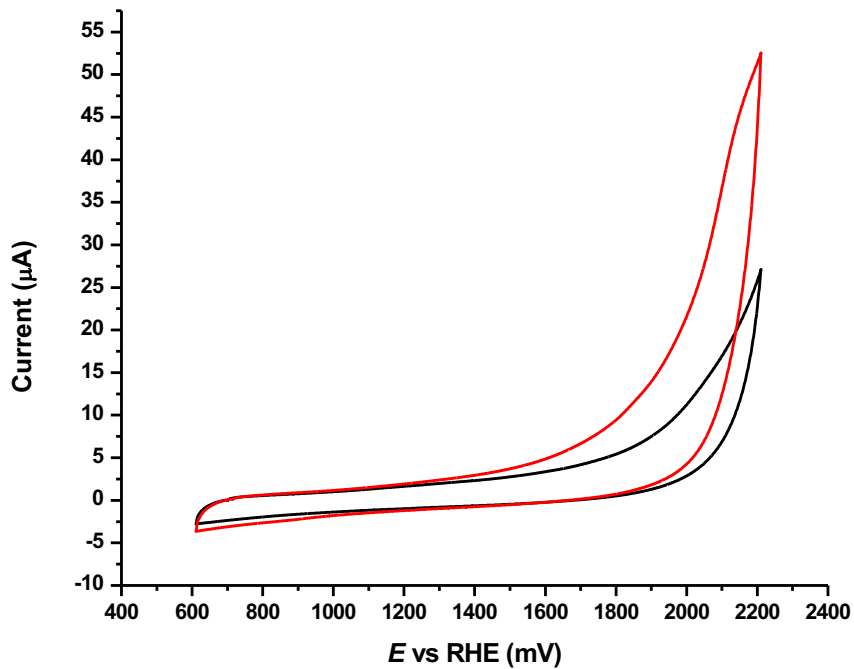


Figure S16. CV of 0.1 M K-Pi buffer pH 7 (black), 0.15 mM **2** in H_2O K-Pi at pH 7 (red). Scan rate = 100 mV s⁻¹.

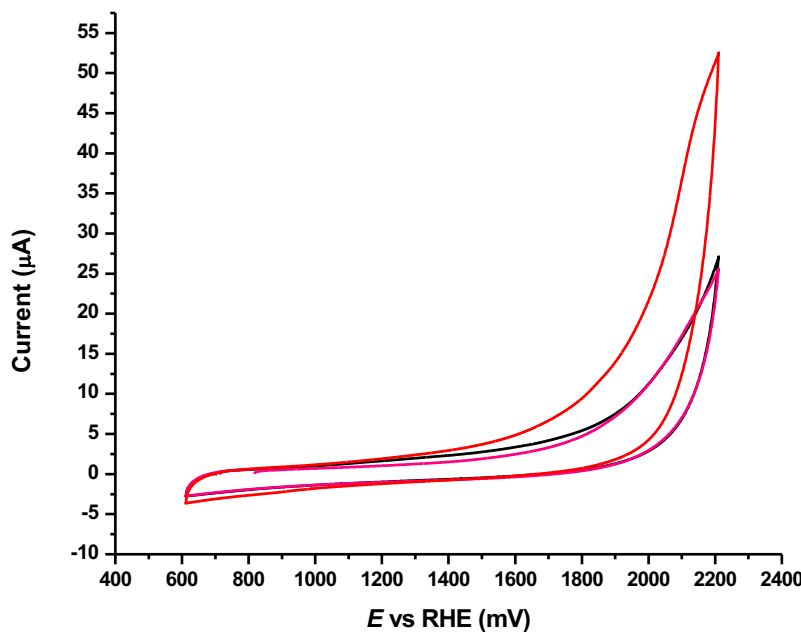


Figure S17. CV of 0.1 M K-Pi buffer pH 7 (black), 0.15 mM **2** in H_2O K-Pi (red). When the working electrode was removed from the catalyst-containing solution without washing and used in a clean buffer solution, no catalytic current was observed (pink). Scan rate = 100 mV s⁻¹.

Overpotential calculation for **2**

Overpotential calculation was carried out at pH7 vs RHE.

$$E \text{ (vs. RHE)} = E_{\text{Ag}/\text{AgCl}} + 0.059 \text{ pH} + E^{\circ}_{\text{Ag}/\text{AgCl}}$$

$$E \text{ (vs. RHE)} = 1.10 + 0.413 + 0.198$$

$$E \text{ (vs. RHE)} = 1.71$$

$$\eta = E \text{ (vs. RHE)} - E^{\circ} \text{ (vs. RHE)} = 1.71 - 0.81 = 0.9 \text{ V} = 900 \text{ mV}$$

Overpotential calculation vs NHE

$$E_{\text{Ag}/\text{AgCl}} = 1.10 \text{ V}$$

$$\eta = E \text{ (vs. NHE)} - E^{\circ} \text{ (vs. NHE)} = 1.39 - 1.23 = 0.16 = 160 \text{ mV}$$

Rate constant calculation for **2**

Data from **Figure S19**, at 100 mV s⁻¹

$$i_{cl} / i_p = 1.38(k_{obs}/v)^{1/2}$$

$$4.74 = 1.38(k_{obs}/v)^{1/2}$$

$$\therefore k_{obs} = 1.18 \text{ s}^{-1}$$

Stability of 1 and 2

Scanning Electron Microscope (SEM) experiments

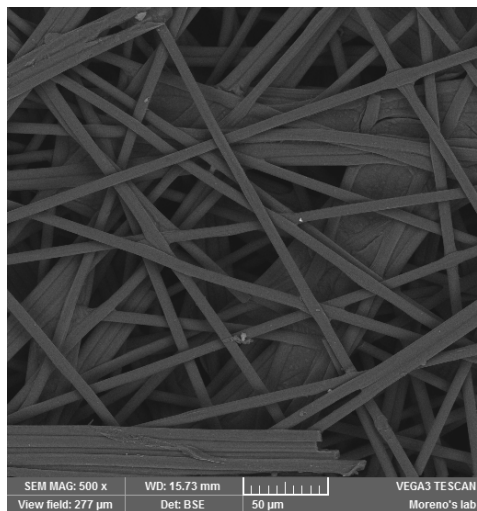


Figure S18. 500x image of graphite electrode before electrolysis (blank).

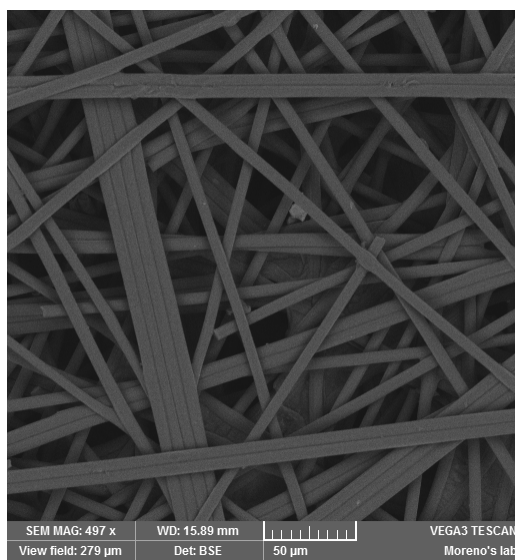


Figure S19. 500x image of graphite electrode after electrolysis experiment of 0.15 mM **1** in 0.1 M H₂O K-Pi pH 7 during 30 min.

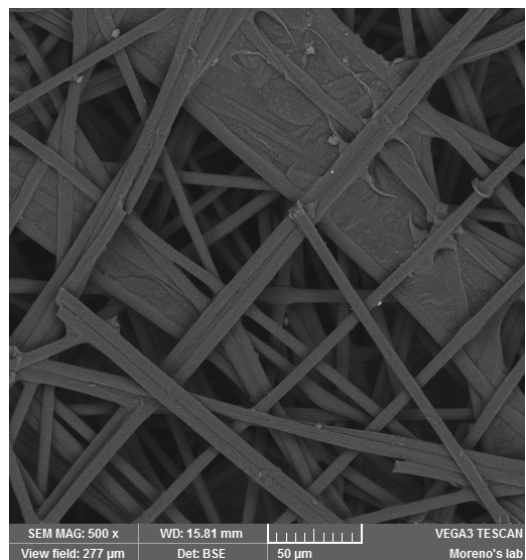


Figure S20. 500x image of graphite electrode after electrolysis experiment of 0.15 mM **2** in 0.1 M H₂O K-Pi pH 7 during 30 min.

UV-vis spectroscopy experiments

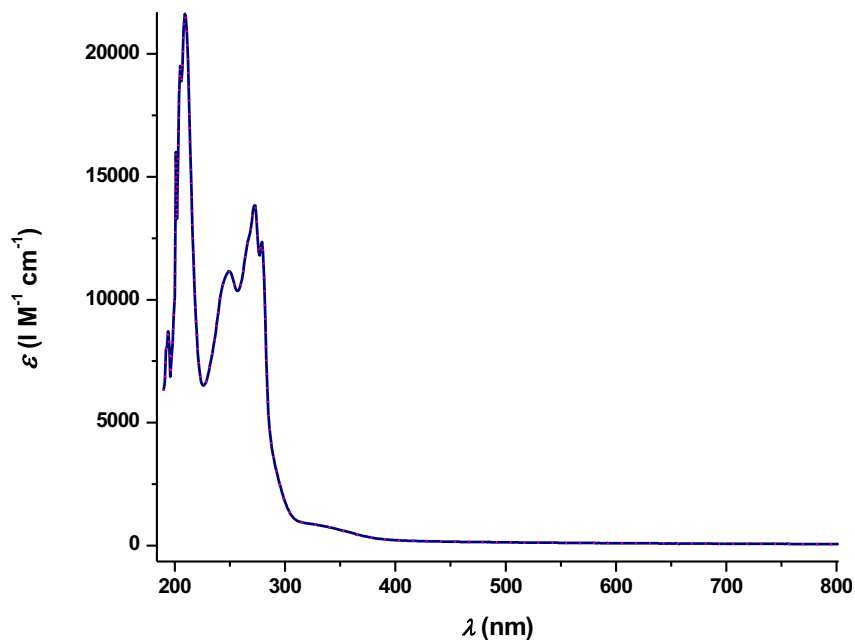


Figure S21. UV-Vis absorption spectra of 0.20 mM **1** in 0.1 M aqueous KPi pH7 before (blue line) and after (pink dotted line) electrolysis for 30 min.

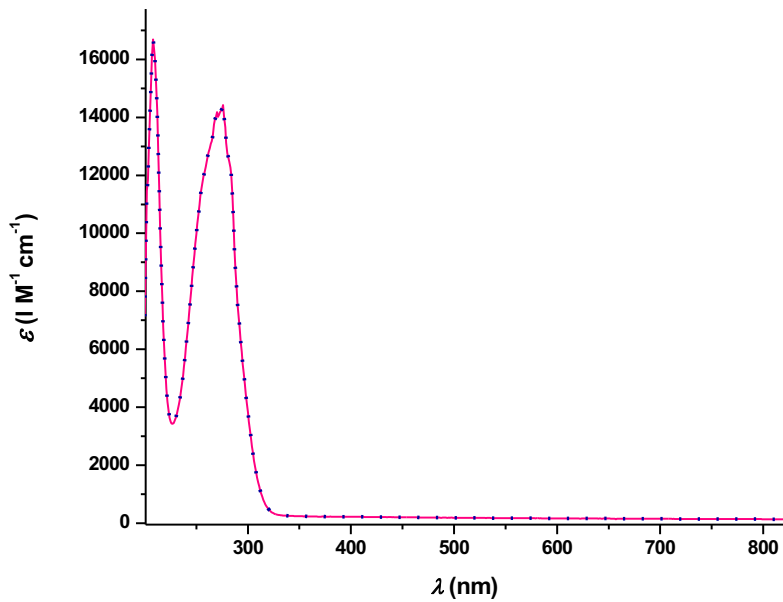


Figure S22. UV-Vis absorption spectra of 0.15 Mm **2** in 0.1 M aqueous KPi pH7 before (blue dotted line) and after (pink) electrolysis for 30 min.

Successive cyclic voltammogram scans of **1** and **2**

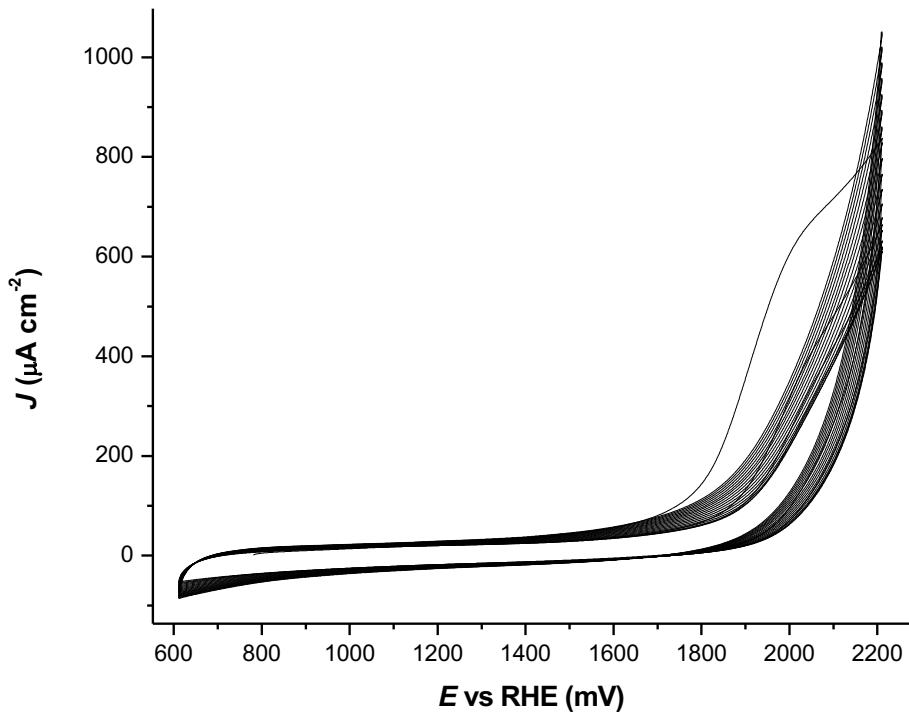


Figure S23. Successive cyclic voltammogram scans of **1**, 0.15 mM 0.1 M pH 7 phosphate buffer with a glassy carbon working electrode, Ag/AgCl reference electrode and Pt counter electrode, scan rate of 100 mV s⁻¹.

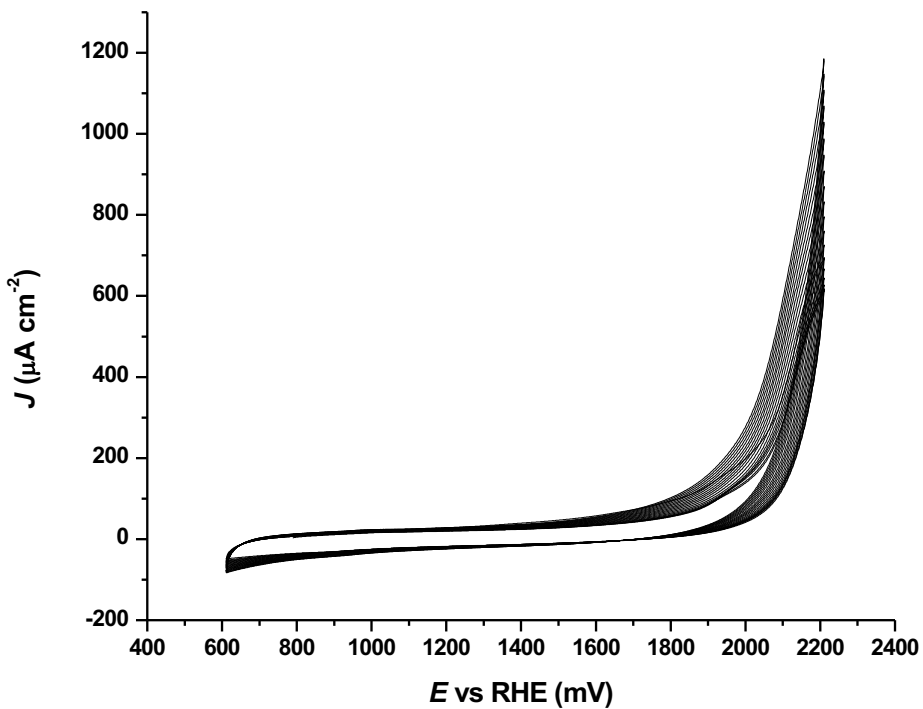


Figure S24. Successive cyclic voltammogram scans of **2**, 0.15 mM 0.1 M pH 7 phosphate buffer with a glassy carbon working electrode, Ag/AgCl reference electrode and Pt counter electrode, scan rate of 100 mV s⁻¹.

Mechanistic Studies

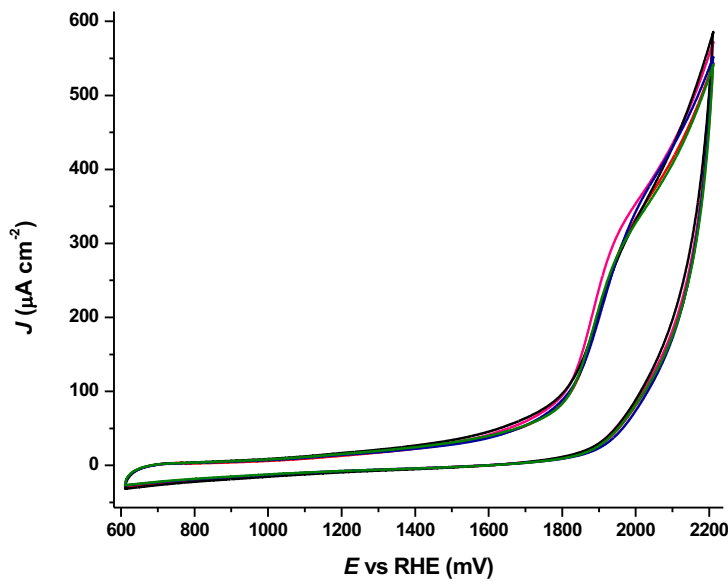


Figure S25. a) CVs of 0.15 mM **1** in K-Pi pH 7 at different concentrations 0.025 M (black), 0.035 M (blue), 0.050 M (red), 0.075 M (green), 0.10 M (pink).

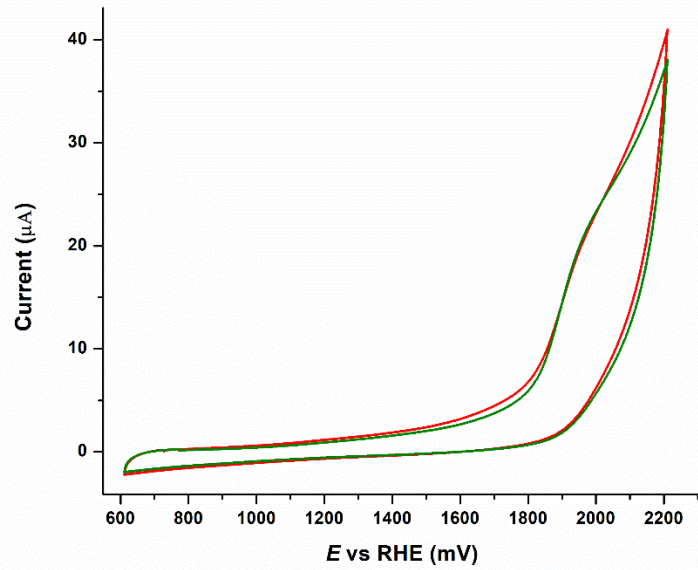


Figure S25. b) CVs of 0.15 mM **1** in K-Pi pH 7 (green) and 0.15 Mm **1** in borate buffer pH 8.5

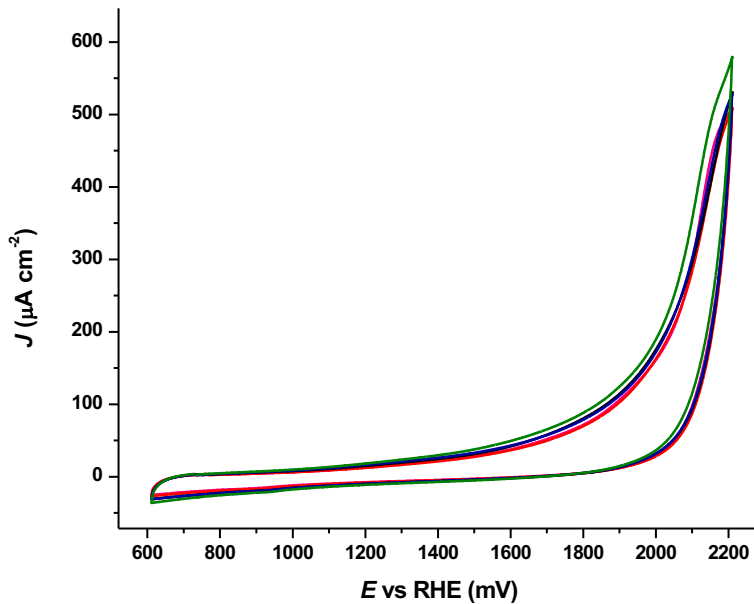


Figure S26. CVs of 0.15 mM **2** in K-Pi pH 7 at different concentrations 0.025 M (black), 0.035 M (blue), 0.050 M (red), 0.075 M (green), 0.10 M (pink).

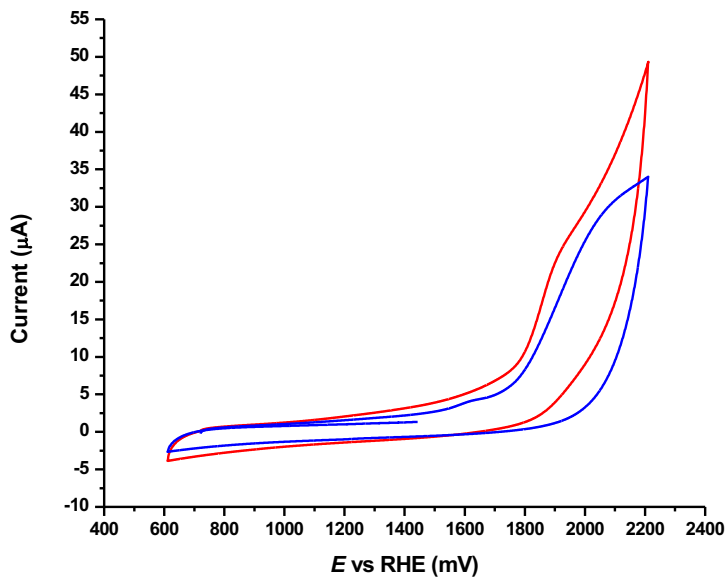


Figure S27. CV of 0.15 mM **1** in K-Pi solution at pH 7 (red), and 0.15 mM **1** in D₂O K-Pi (blue). Scan rate = 100 mV s⁻¹.

Kinetic Isotope Effect calculation for **1**

A secondary isotope effect can be afforded with KIE = 0.7-1.5.^{29,31}

$$\text{KIE} = k_{cat, H_2O} / k_{cat, D_2O} = (i_{cat, H_2O} / i_{cat, D_2O})^2$$

$$\text{KIE} = 0.70$$

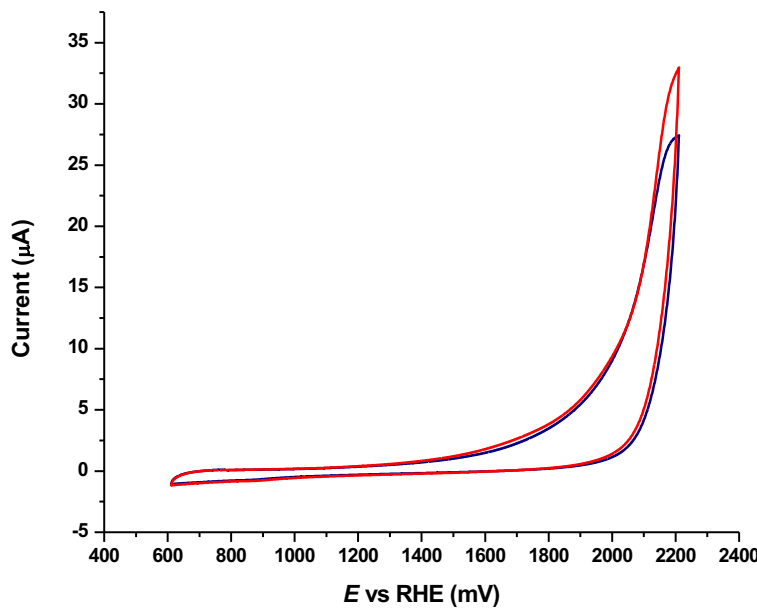


Figure S28. CV of 0.1 M K-Pi buffer pH 7 (black), 0.15 mM **2** in H₂O (red), 0.15 mM **2** in D₂O (blue). Scan rate = 100 mV s⁻¹.

Kinetic Isotope Effect calculation for **2**

$$\text{KIE} = k_{cat, H_2O} / k_{cat, D_2O} = (i_{cat, H_2O} / i_{cat, D_2O})^2$$

$$\text{KIE} = 1.4$$

Electrochemical data for 3

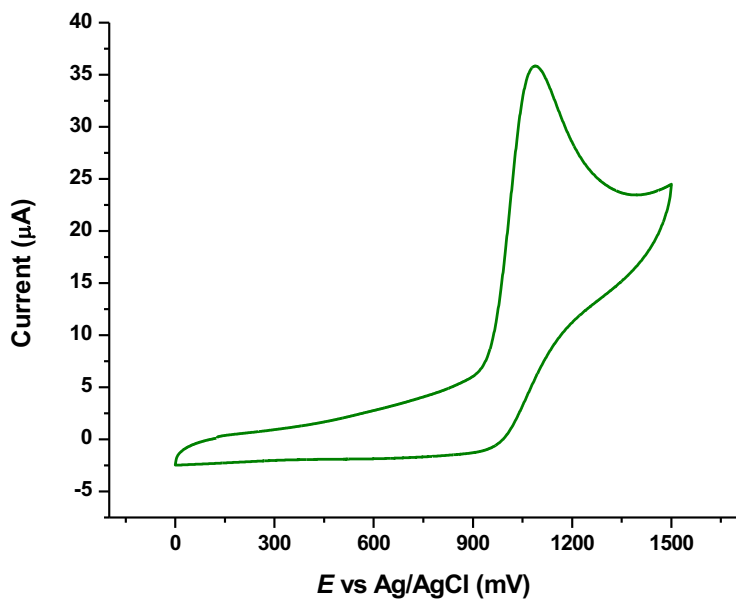


Figure S29. CV of 3 in DMF.

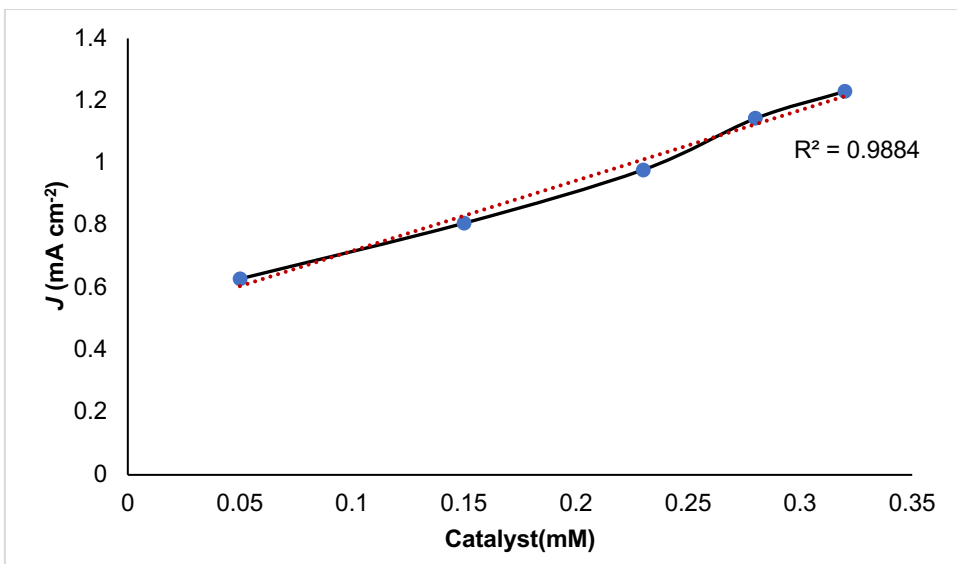


Figure S30. Catalytic current as a function of the catalyst concentration from 0.05 to 0.32 mM measured in 0.1 M K-Pi buffer pH 7. Red line represents the best linear fit up to [3].

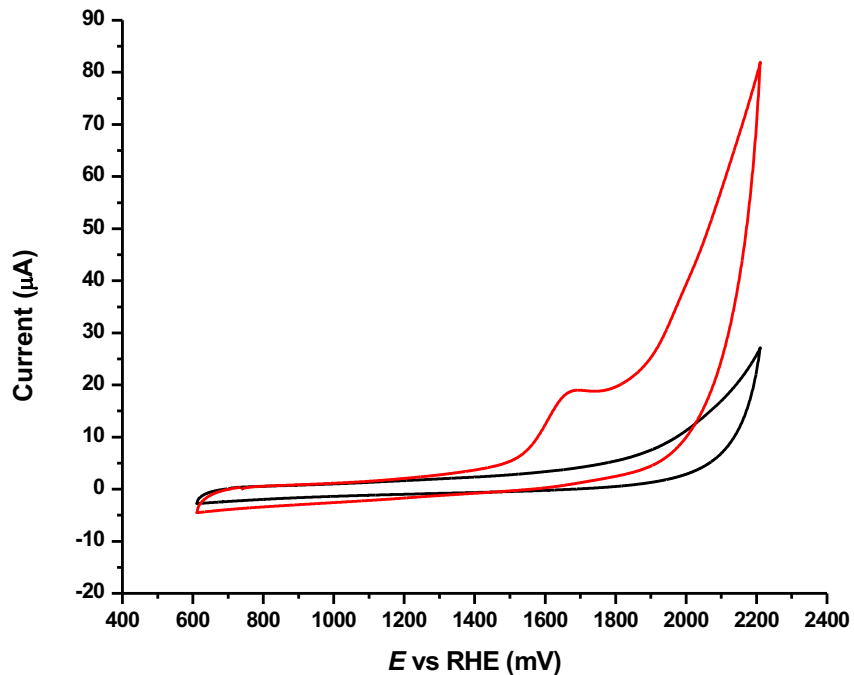


Figure S31. CV of 0.1 M K-Pi pH 7 (black), 0.28 mM 3 in H₂O K-Pi (red). Scan rate = 100 mV s⁻¹.

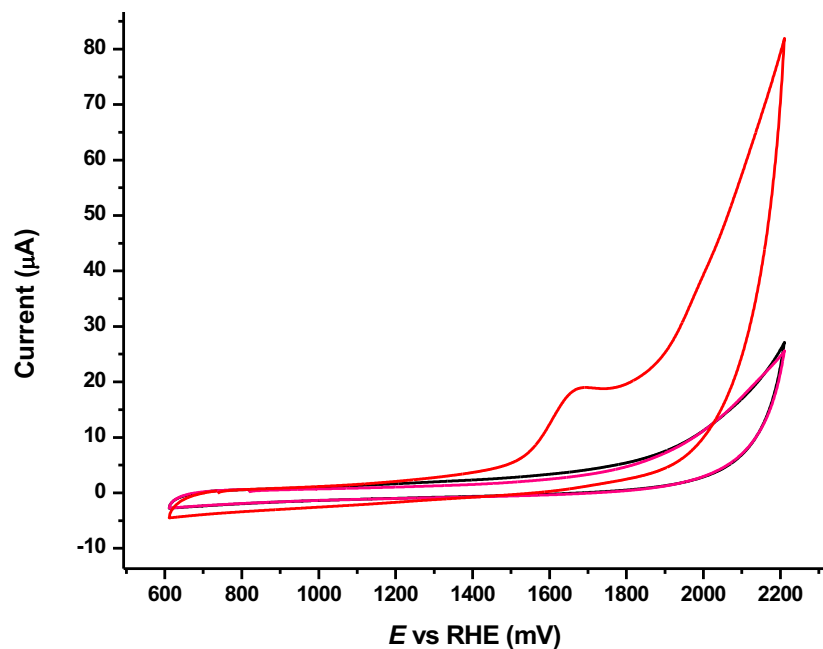


Figure S32. CV of 0.1 M K-Pi buffer pH 7 (black), 0.28 mM 3 in H₂O K-Pi (red). When the working electrode was removed from the catalyst-containing solution without washing and used in a clean buffer solution, no catalytic current was observed (pink). Scan rate = 100 mV s⁻¹.

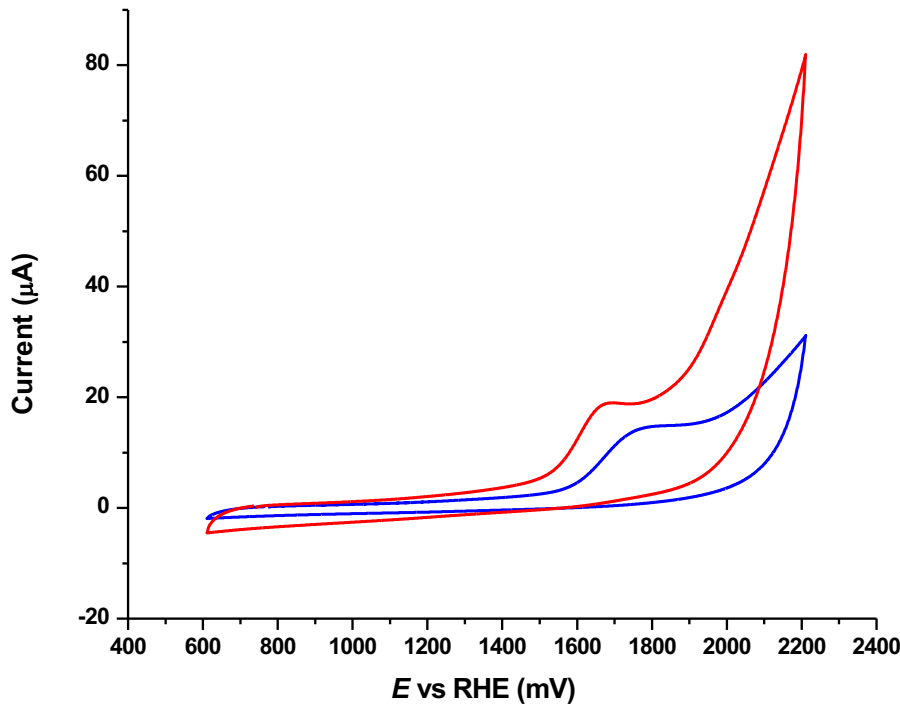


Figure S33. CV of 0.28 mM **3** in K-Pi at pH 7 (red), and 0.28 mM **3** in D₂O K-Pi (blue). Scan rate = 100 mV s⁻¹.

Overpotential calculation for **3**

Overpotential at pH7 vs RHE.

$$E(\text{vs. RHE}) = E_{\text{Ag}/\text{AgCl}} + 0.059 \text{ pH} + E^{\circ}_{\text{Ag}/\text{AgCl}}$$

$$E(\text{vs. RHE}) = 1.2 + 0.413 + 0.198$$

$$E(\text{vs. RHE}) = 1.81 - 0.81$$

$$\eta = E(\text{vs. RHE}) - E^{\circ}(\text{vs. RHE}) = 1.81 - 0.81 = 1.0 \text{ V} = 1000 \text{ mV}$$

Rate constant calculation for **3**

Data from **Figure S26**, at 100 mV s⁻¹

$$i_{cl} i_p = 1.38(k_{obs}/v)^{1/2}$$

$$3.93 = 1.38(k_{obs}/v)^{1/2}$$

$$\therefore k_{obs} = 8.11 \text{ s}^{-1}$$

Kinetic Isotope Effect calculation for **3**

$$\text{KIE} = k_{cat, H_2O} / k_{cat, D_2O} = (i_{cat, H_2O} / i_{cat, D_2O})^2$$

$$\text{KIE} = 1.7$$

Dioxygen quantification

Dioxygen quantification for **1**

Table S4. Dioxygen concentration electrochemically generated by **1**.

	Time	O ₂ concentration (mg/L)
Buffer K-Pi pH7 0.1M	0	0
Buffer K-Pi pH7 + 1	16.7 min	≈0.48
Buffer K-Pi pH7 + 1	120 min	4.14

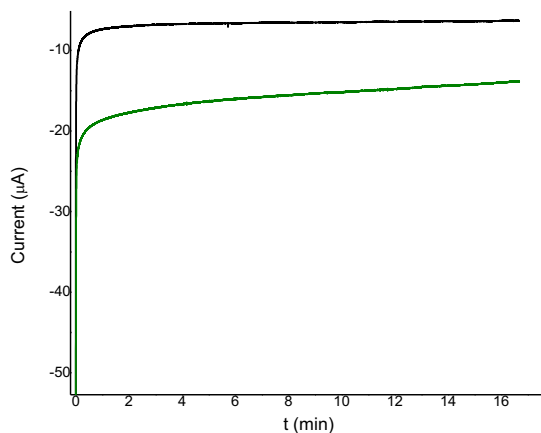


Figure S34. Controlled potential electrolysis at 1.5 V of 0.15 mM **1** in K-Pi at pH 7 (green), K-Pi pH 0.1M (black).

Dioxygen quantification for **2**

Table S5. Dioxygen concentration electrochemically generated by **2**.

	Time	O ₂ concentration (mg/L)
Buffer K-Pi pH 7 0.1M	0	0
Buffer K-Pi pH 7 + 2	16.7 min	≈0.72
Buffer K-Pi pH 7 + 2	120 min	6.31

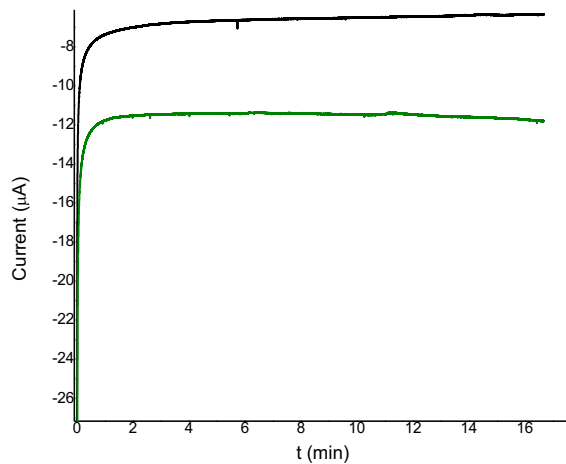


Figure S35. Controlled potential electrolysis at 1.6 V of 0.15 mM **2** in K-Pi at pH 7 (green), K-Pi pH 0.1M (black).

Dioxygen quantification for **3**

Table S6. Dioxygen concentration electrochemically generated by **3**.

	Time	O ₂ concentration (mg/L)
Buffer K-Pi pH 7 0.1M	0	0
Buffer K-Pi pH 7 + 3	16.7 min	≈0.41
Buffer K-Pi pH 7 + 3	120 min	3.28

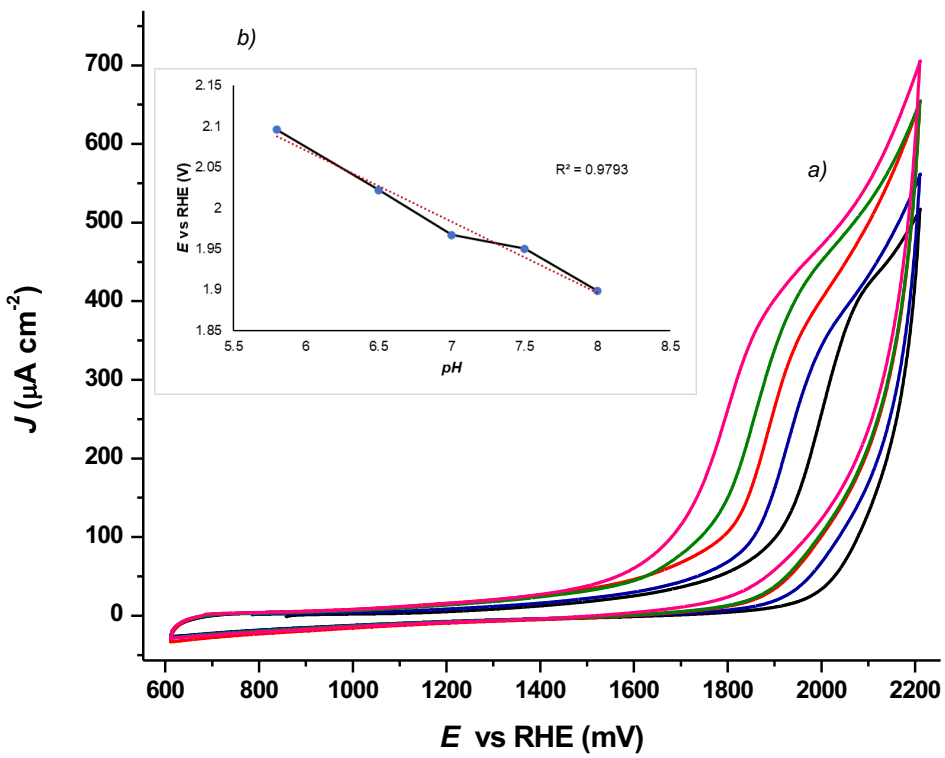


Figure S36. a) CVs of 0.15 mM **1** in K-Pi solution at different pH values 5.8 (black), 6.5 (blue), 7.0 (red), 7.5 (green), 8.0 (pink). b) Plot of potential versus pH.

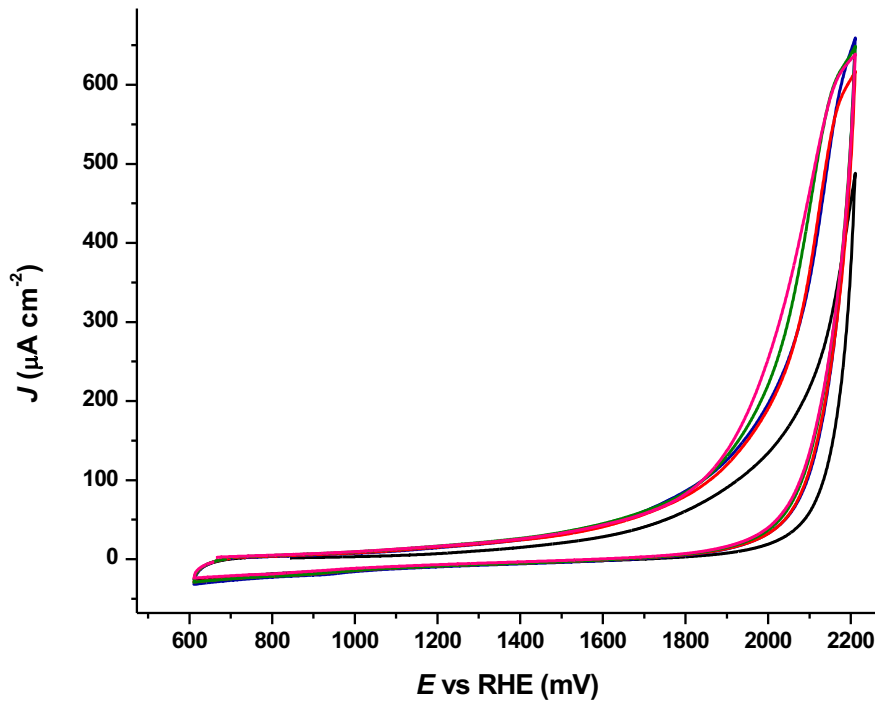


Figure S37. CVs of 0.15 mM **2** in K-Pi solution at different pH values 5.8 (black), 6.5 (blue), 7.0 (red), 7.5 (green), 8.0 (pink).

DFT Calculations

$[(\mu_3\text{-}1\text{-H}\text{-}2\text{-benzimidazole}\text{-CH}_2\text{O})\text{NiCl}(\text{MeOH})]_4$, complex 1

FULL STRUCTURE OPTIMIZATION OF 1 IN WATER

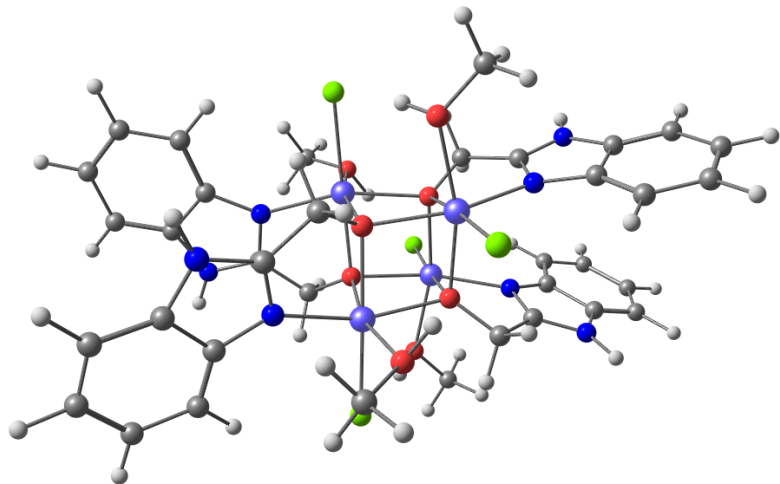
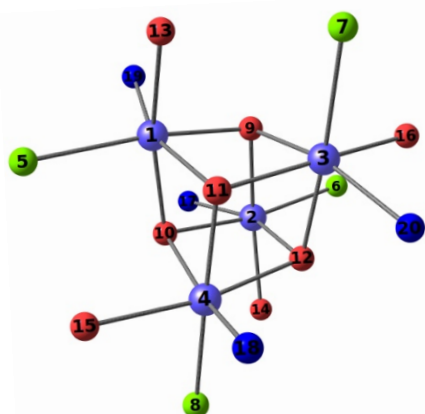


Figure S38. Optimized structure of complex 1 in water.

The standard deviations are in the range of the DFT precision at 0.043 Å and 1.6° for bond lengths and angles, respectively.

Table S7. Bond length differences between experimental and calculated 2 in water.

	exptl	calcd	Δ distance	(calcd-exptl) ²
Ni1O9	2.073	2.105	0.032	0.001024
Ni1O10	2.034	2.090	0.056	0.003136
Ni1O11	2.089	2.137	0.048	0.002304
Ni1O13	2.099	2.157	0.058	0.003364
Ni1Cl5	2.436	2.407	-0.029	0.000841
Ni1N19	2.038	2.050	0.012	0.000144
Ni2O9	2.050	2.088	0.038	0.001444
Ni2O10	2.117	2.135	0.018	0.000324
Ni2O12	2.094	2.160	0.066	0.004356
Ni2O14	2.081	2.102	0.021	0.000441
Ni2Cl6	2.370	2.406	0.036	0.001296
Ni2N17	2.070	2.051	-0.019	0.000361
Ni3O9	2.078	2.103	0.025	0.000625
Ni3O11	2.101	2.090	-0.011	0.000121
Ni3O12	2.073	2.161	0.088	0.007744
Ni3O16	2.081	2.136	0.055	0.003025
Ni3C17	2.358	2.412	0.054	0.002916
Ni3N20	2.082	2.049	-0.033	0.001089
Ni4O10	2.096	2.135	0.039	0.001521
Ni4O11	2.081	2.104	0.023	0.000529
Ni4O12	2.103	2.161	0.058	0.003364
Ni4O15	2.040	2.086	0.046	0.002116
Ni4C18	2.382	2.410	0.028	0.000784
Ni4N18	2.043	2.046	0.003	0.000009



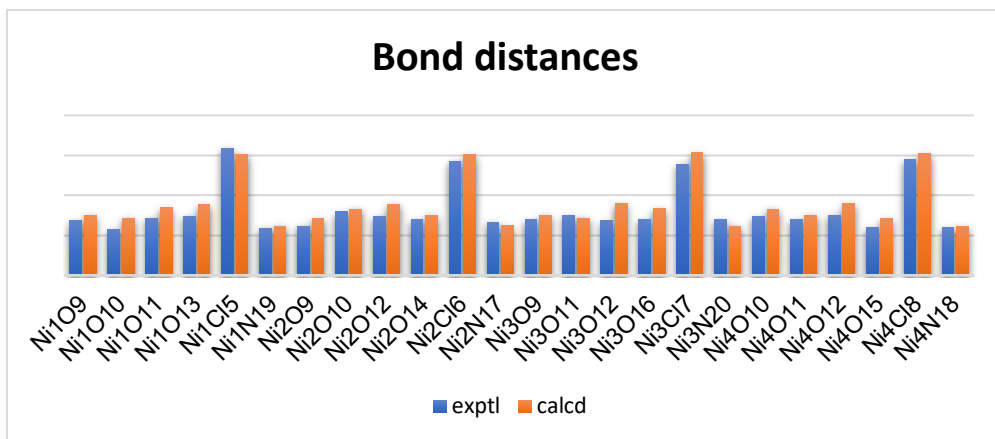


Figure S39. Distances around Ni(II) for the optimized complex **1** in water.

Table S8. Angle difference between experimental and calculated **1** in water.

	ANGLES								
	exptl	calcd	Δ °	(calcd-exptl) ²		exptl	calcd	Δ °	(calcd-exptl) ²
O9Ni1O10	80.8	81.3	-0.5	0.25	O9Ni3O11	79.8	81.6	-1.8	3.24
O9Ni1O11	80.8	78.6	2.2	4.84	O9Ni3O12	93.6	97.0	-3.4	11.56
O9Ni1O13	96.3	96.7	-0.4	0.16	O9Ni3O16	80.5	78.6	1.9	3.61
O9Ni1N19	80.7	80.1	0.6	0.36	O9Ni3N20	78.8	80.1	-1.3	1.69
O9Ni1Cl5	174.4	174.1	0.3	0.09	O9Ni3Cl7	175.3	174.1	1.2	1.44
O10Ni1O11	81.1	80.7	0.4	0.16	O11Ni3O12	86.6	84.5	2.1	4.41
O10Ni1O13	84.3	84.5	-0.2	0.04	O11Ni3O16	80.9	80.7	0.2	0.04
O10Ni1N19	160.5	160.2	0.3	0.09	O11Ni3N20	158.1	160.6	-2.5	6.25
O10Ni1Cl5	99.0	98.2	0.8	0.64	O11Ni3Cl7	99.7	98.1	1.6	2.56
O11Ni1O13	165.4	165.0	0.4	0.16	O12Ni3O16	167.0	165.0	2	4
O11Ni1N19	102.1	102.0	0.1	0.01	O12Ni3N20	89.8	91.2	-1.4	1.96
O11Ni1Cl5	93.6	95.5	-1.9	3.61	O12Ni3Cl7	91.0	88.8	2.2	4.84
O13Ni1N19	91.5	91.1	0.4	0.16	O16Ni3N20	100.4	102.0	-1.6	2.56
O13Ni1Cl5	89.3	89.1	0.2	0.04	O16Ni3Cl7	94.8	95.6	-0.8	0.64
N19Ni1Cl5	100.0	101.0	-1	1	N20Ni3Cl7	102.0	100.8	1.2	1.44
O9Ni2O10	79.4	80.7	-1.3	1.69	O10Ni4O11	80.4	78.6	1.8	3.24
O9Ni2O12	85.0	84.4	0.6	0.36	O10Ni4O12	166.4	164.9	1.5	2.25
O9Ni2O14	81.7	78.6	3.1	9.61	O10Ni4O15	81.6	80.7	0.9	0.81
O9Ni2N17	159.0	160.3	-1.3	1.69	O10Ni4N18	99.5	101.9	-2.4	5.76
O9Ni2Cl6	98.6	98.2	0.4	0.16	O10Ni4Cl8	96.8	95.8	1	1
O10Ni2O12	164.3	164.9	-0.6	0.36	O11Ni4O12	91.7	96.7	-5	25
O10Ni2O14	79.6	78.6	1	1	O11Ni4O15	82.3	81.5	0.8	0.64
O10Ni2N17	104.5	102.2	2.3	5.29	O11Ni4N18	80.2	80.2	0	0
O10Ni2Cl6	95.0	95.4	-0.4	0.16	O11Ni4Cl8	177.2	174.4	2.8	7.84
O12Ni2O14	96.4	97.0	-0.6	0.36	O12Ni4O15	86.4	84.4	2	4
O12Ni2N17	89.5	91.2	-1.7	2.89	O12Ni4N18	90.0	91.3	-1.3	1.69
O12Ni2Cl6	89.1	89.0	0.1	0.01	O12Ni4Cl8	90.9	88.8	2.1	4.41
O14Ni2N17	78.8	80.1	-1.3	1.69	O15Ni4N18	162.1	160.6	1.5	2.25
O14Ni2Cl6	174.5	173.9	0.6	0.36	O15Ni4Cl8	96.8	98.0	-1.2	1.44
N17Ni2Cl6	101.6	100.9	0.7	0.49	N18Ni4Cl8	100.8	100.9	-0.1	0.01

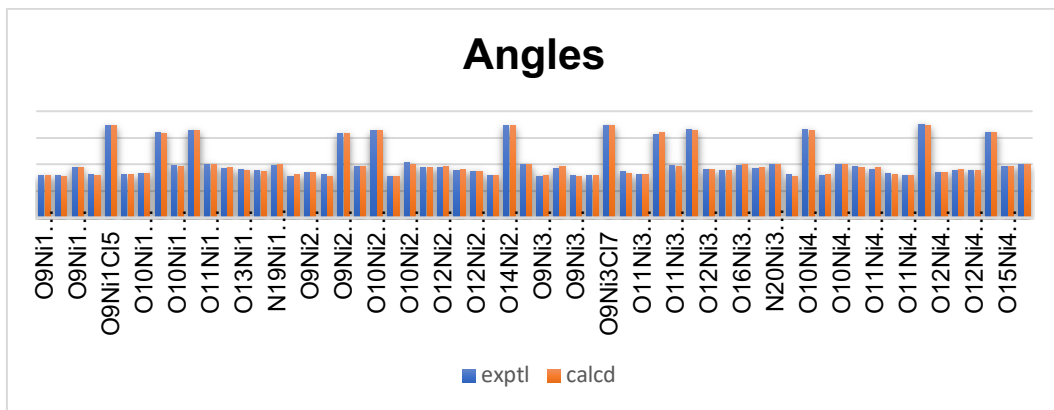


Figure S40. Angles around Ni(II) for the optimized **1** in water.

SPIN DENSITY PLOTS

From Mulliken spin population analysis, we observe that 92% of the spin density is found at the Ni(II) metal centers as expected in the case of a tetranuclear complex with four high spin Ni(II) ions ($S=1$ each).

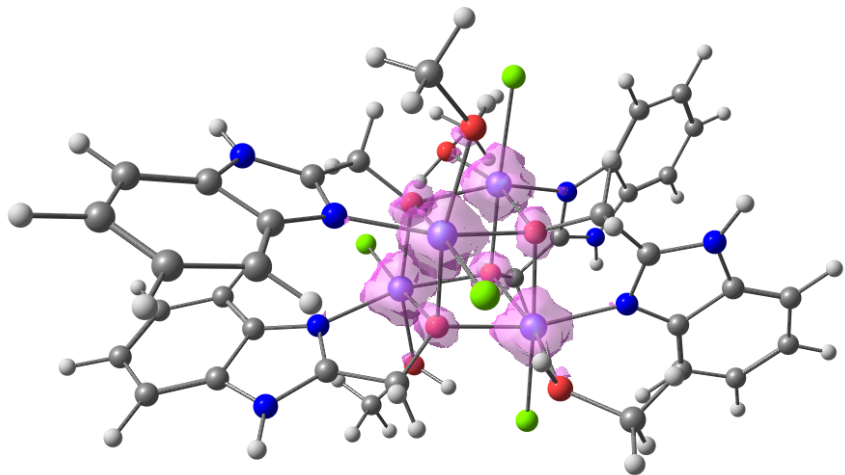


Figure S41. Spin density of optimized complex **1** in water.

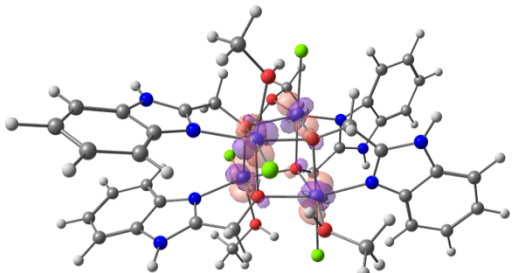
Table S9. Mulliken atomic charges and spin population for complex **1** in water.

Atom	Spin population
Ni	1.540647
Ni	1.540561
Ni	1.540611
Ni	1.540392
Cl	0.086363
Cl	0.086408
Cl	0.086639
Cl	0.086254
O	0.217160
O	0.216738
O	0.217019
O	0.216571

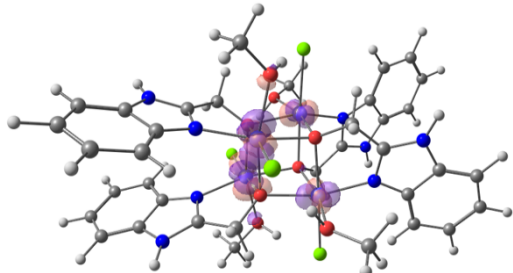
SINGLY OCCUPIED MOLECULAR ORBITALS

The singly occupied molecular orbitals are mainly metal based and consistent with the description of a tetranuclear complex with 4 high spin Ni(II) centers.

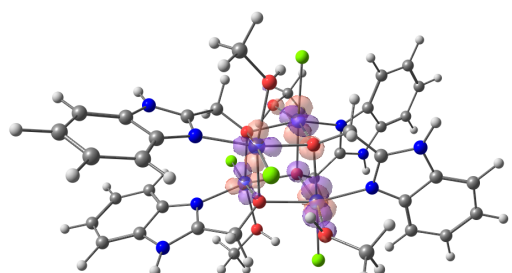
-5.5936 eV



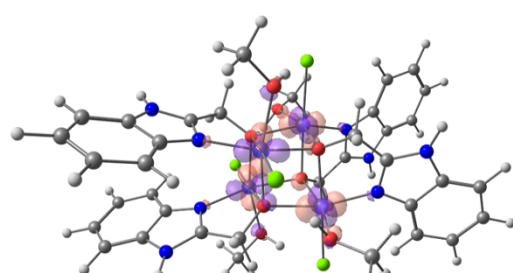
-5.5905 eV



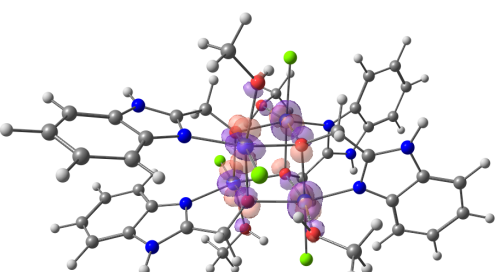
-5.4933 eV



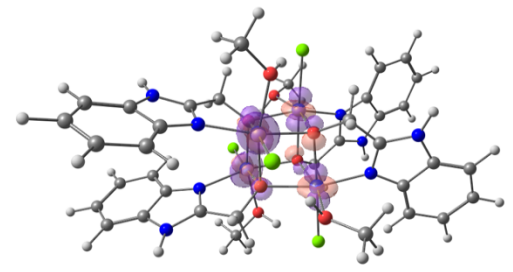
-5.0282 eV



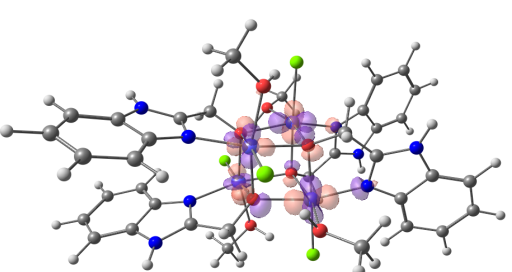
-4.9677 eV



-4.8848 eV



-4.8838 eV



-4.8825 eV

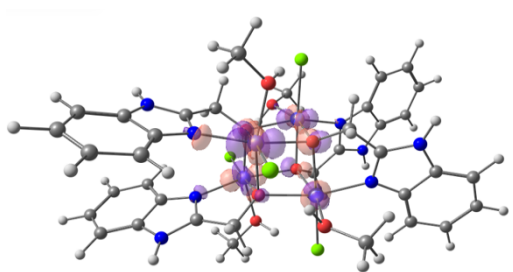


Figure S42. Singly occupied molecular orbitals of **1** in water.

OPTICAL PROPERTIES

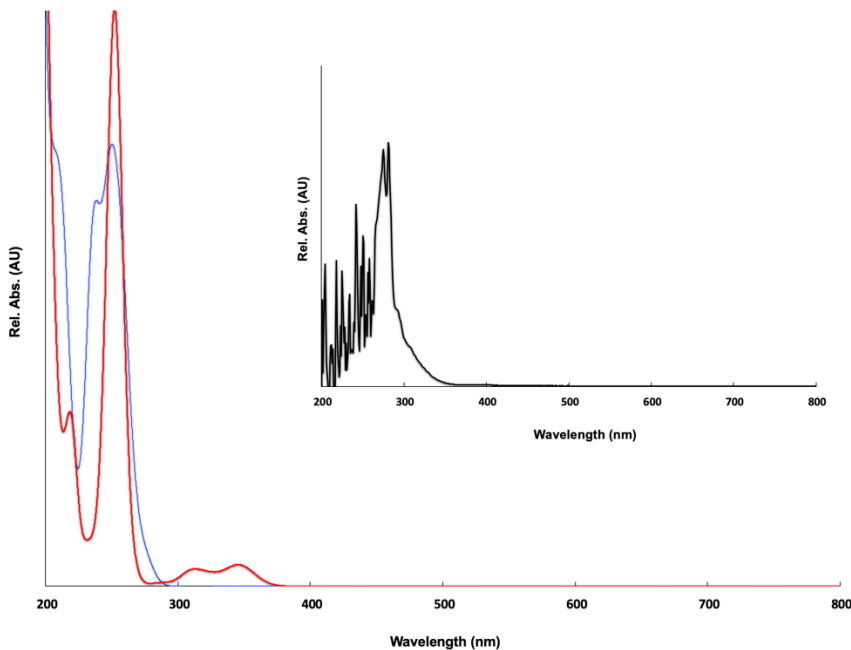


Figure S43. Theoretical fit of the UV-vis spectra of complexes **1** (red line) and **3** (blue line) and comparison with the experimental data (black line).

TD-DFT calculations were carried out to predict the UV-vis features of complexes **1** and **3**. Our calculations using the optimized structure of complex **1** adequately reproduce the main spectral features of the experimental spectrum with two main bands in the [235-250 nm] range and no absorption band in the low-energy region. Comparison of the computed spectra with the experimental one thus supports that the species present in solution is compatible with the tetranuclear complex **1**.

Table S10. Theoretical assignments of the main bands for complexes **1** and **3**

Complex	Wavelength, λ^{calc} (nm)	Oscillator strength, f^{calc}
1	237	0.023
	249	0.030
3	252	0.035
	310	0.009
	347	0.008

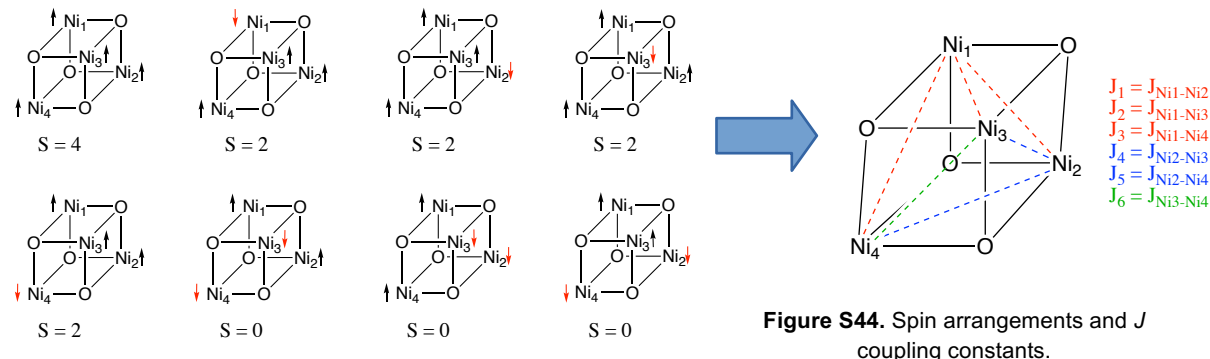
MAGNETIC PROPERTIES

Broken symmetry

The cubanes have four Ni(II) centers that we assume are in high spin configuration, thus each having two unpaired electrons. Magnetic interactions between these paramagnetic centers are to be expected and can be described by the exchange coupling constant, J . This parameter describes the strength and nature of the magnetic interactions, with antiferromagnetic coupling expected for negative J values and ferromagnetic interaction leading to positive ones. The prediction of the J values in polynuclear transition metal complexes can be conducted using the “broken symmetry” approach within the density functional theory (DFT) framework.¹³⁻¹⁵ While the calculation of high spin states is straightforward using DFT because they can be described by a single determinant, it is not the case for the low spin states which are multiconfigurational. The broken symmetry is then a mathematical tool to evaluate the energy of the

low spin states as this approach allows the spin-up and spin-down electrons to be localized on different areas of the molecule so that they can be coupled magnetically but are not forcibly paired.

In principle, the number of spin arrangement expected is 2^{n-1} , so for complexes **1** and **2** there are eight different spin configurations which result in six J constants, Figure S44.



Our results indicate that the coupling scheme in the cubanes is rather weak and overall ferromagnetic interactions are operative between the paramagnetic centers. It also shows that the lowest energy configuration is the high spin one, and so it constitutes the ground spin state of the systems.

Table S11. Calculated exchange coupling constants J, and Ni-O-Ni angles for **1** in water.

	Energies (Eh)	ΔE (Eh)	ΔE (cm^{-1})		Eh	cm^{-1}
$\alpha\alpha\alpha$	-10312.065583	0.000000	0			
$\alpha\alpha\beta$	-10312.065428	0.000155	34	$J_{1-\text{AB}}$	0.000015	3.29
$\alpha\alpha\beta\alpha$	-10312.065431	0.000152	33	$J_{2-\text{AC}}$	0.000015125	3.32
$\alpha\beta\alpha\alpha$	-10312.065431	0.000152	33	$J_{3-\text{AD}}$	0.000007875	1.73
$\beta\alpha\alpha\alpha$	-10312.065431	0.000152	33	$J_{4-\text{BC}}$	0.0000075	1.65
$\alpha\beta\beta\alpha$	-10312.065339	0.000244	54	$J_{5-\text{BD}}$	0.000007875	1.73
$\alpha\beta\alpha\beta$	-10312.065400	0.000183	40	$J_{6-\text{CD}}$	0.0000155	3.40
$\alpha\alpha\beta\beta$	-10312.065399	0.000184	40			

Angles

Ni1O5Ni2	98.3
Ni1O5Ni4	101.1
Ni1O6Ni2	97.3
Ni1O6Ni3	98.2
Ni1O7Ni3	97.2
Ni1O7Ni4	101.1
Ni2O5Ni4	97.2
Ni2O6Ni3	101.1
Ni2O8Ni3	101.1
Ni2O8Ni4	98.2
Ni3O7Ni4	98.3
Ni3O8Ni4	97.2

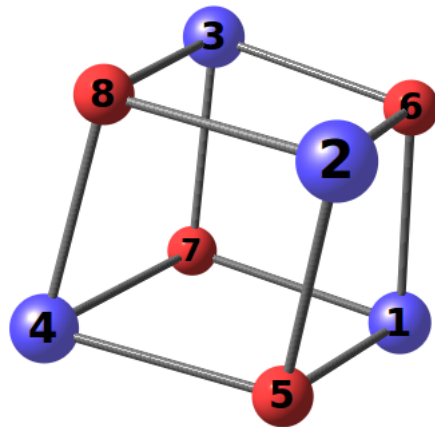


Table S12. Spin ladder of the optimized complex **1** in water.

Spin states	Energy (cm^{-1})
S = 4	0
S = 3	15.6
S = 3	20.1
S = 3	24.8
S = 2	27.9
S = 2	31.7

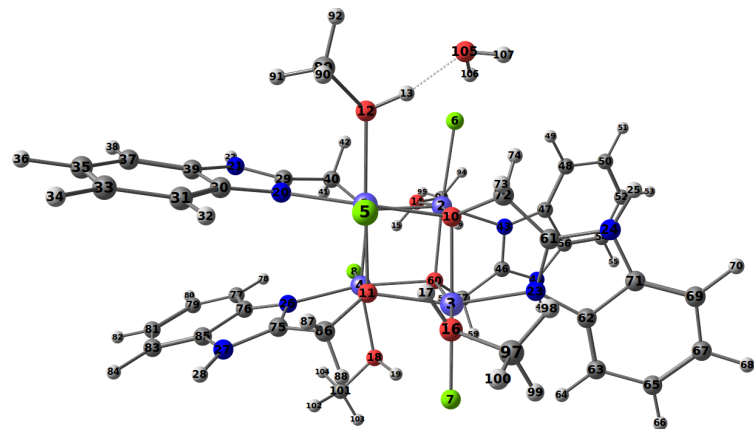
LIGAND EXCHANGE

Relaxed surface scan

We investigated the dissociation of a MeOH (centers 12, 13, 80, 91, 92) molecule from a Ni center (center 1), and substitution by a water (center 105, 106, 107) molecule.

a. H₂O – MeOH exchange

A)



B)

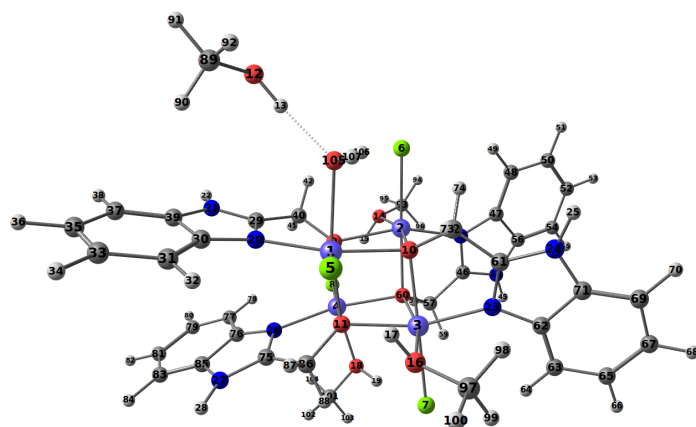


Figure S45. Relaxed surface scan: A) Ni₁-H₂O distance = 4.15 Å, B) Ni₁-H₂O distance = 2.33 Å.

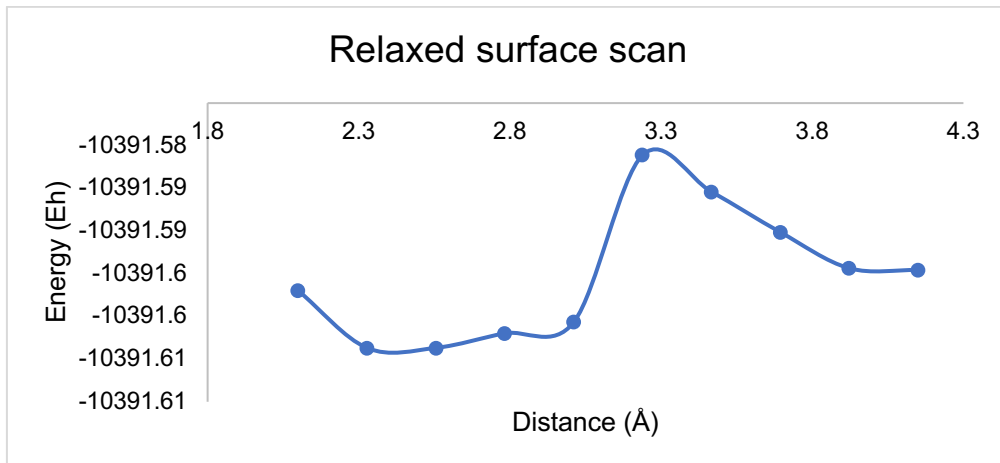


Figure S46. Relaxed surface scan of **1** for bond distance between Ni₁ (center 1) and H₂O (centers 105, 106 and 107).

Table S13. Relaxed surface scan of bond length between atoms 1 (Ni₁) and 105 (O) from 4.15 Å to 2.10 Å in 10 steps.

Bond length (Å)	Energy (Eh)
4.15	-10391.5945677002
3.92	-10391.5943478985
3.69	-10391.5901240968
3.47	-10391.5853904972
3.24	-10391.5810937026
3.01	-10391.6006700706
2.78	-10391.601973866
2.56	-10391.6036821771
2.33	-10391.6036970663
2.10	-10391.5969890919

Numerical frequency calculations were performed using both the initial step and minimum energy point of the relaxed surface scan (S46), for which the H₂O molecule is at 4.15 Å and 2.33 Å from the Ni center respectively. A Gibbs free energy difference of -7.1 kcal mol⁻¹ was obtained supporting the feasibility of the ligand exchange process (Table S14).

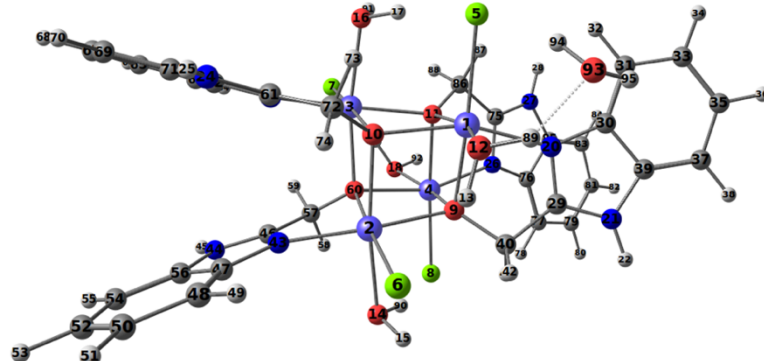
Table S14. Gibbs free energy ligand exchange for complex **1** in water.

Free Gibbs energy (Eh)	
Complex 1 with H ₂ O at 2.33 Å	-10390.91447738
Complex 1 with H ₂ O at 4.15 Å	-10390.90322973
Δ Free Gibbs energy (Eh)	-0.01124765
Δ Free Gibbs energy (kcal.mol ⁻¹)	-7.1

b. H₂O – Cl exchange

After the MeOH-H₂O exchange, we investigated the dissociation of a Cl (center 5) from a Ni center (center 1) and the formation of a bond between the metal and an external water molecule (centers 93, 94 and 95).

A)



B)

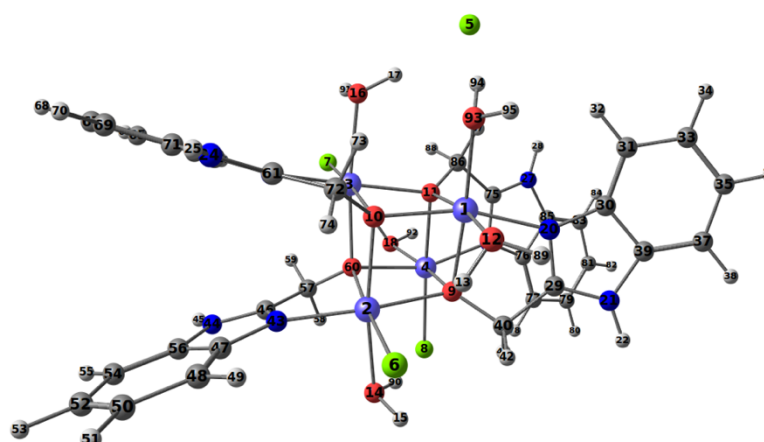


Figure S47. Relaxed surface scan: A) Ni₁-H₂O distance = 3.86 Å, B) Ni₁-H₂O distance = 2.10 Å.

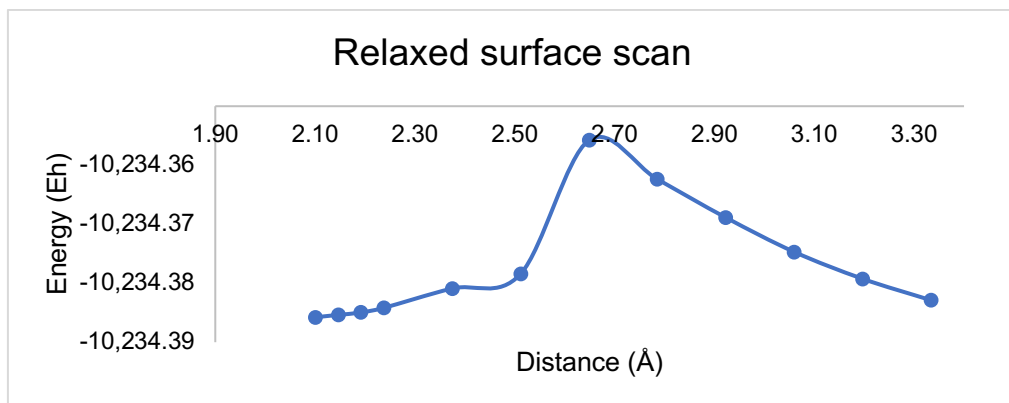


Figure S48. Relaxed surface scan of complex **1** for bond distance between Ni₁ (center 1) and H₂O (centers 93, 94 and 95).

Table S15. Relaxed surface scan of bond length between atoms 1 (Ni_1) and 93 (O) from 3.86 Å to 2.10 Å in 10 steps.

Bond lenght (Å)	Energy (Eh)
3.33	-10234.3828775551
3.20	-10234.3792441832
3.06	-10234.3746832157
2.92	-10234.3688568824
2.79	-10234.3623603392
2.65	-10234.3557914026
2.51	-10234.3784647549
2.37	-10234.3808945767
2.24	-10234.3841874243
2.19	-10234.3849724208

Numerical frequency calculations were performed using both the initial and final steps of the relaxed surface scan (Figure S47), for which the H_2O molecule is at 3.33 Å and 2.10 Å from the Ni center respectively. A Gibbs free energy difference of 2.8 kcal mol⁻¹ was obtained, supporting the feasibility of the ligand exchange process (Table S16).

Table S16. Gibbs free energy ligand exchange for complex **1** in water.

Free Gibbs energy (Eh)	
Complex 2 with H_2O at 2.10 Å	-10233.79284072
Complex 2 with H_2O at 3.33 Å	-10233.79729420
Δ Free Gibbs energy (Eh)	0.00445348
Δ Free Gibbs energy (kcal.mol ⁻¹)	2.8

OXIDATION

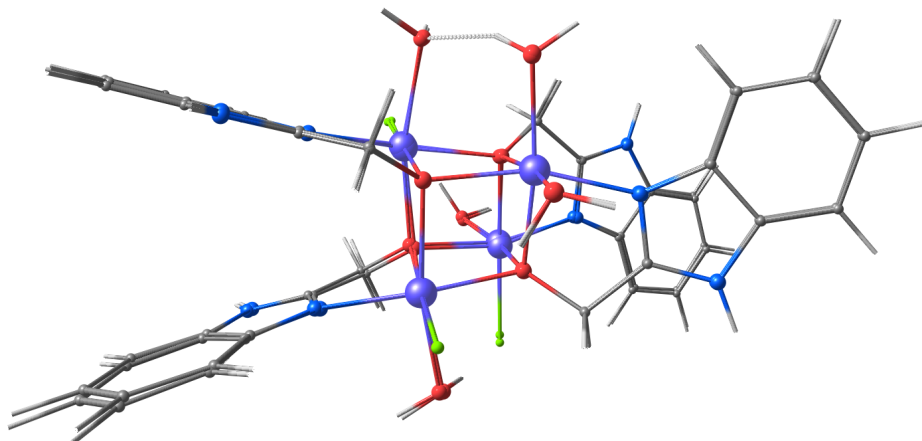


Figure S49. Superimposition of DFT-optimized structures of water-substituted complex **1** before and after oxidation at Ni_1 .

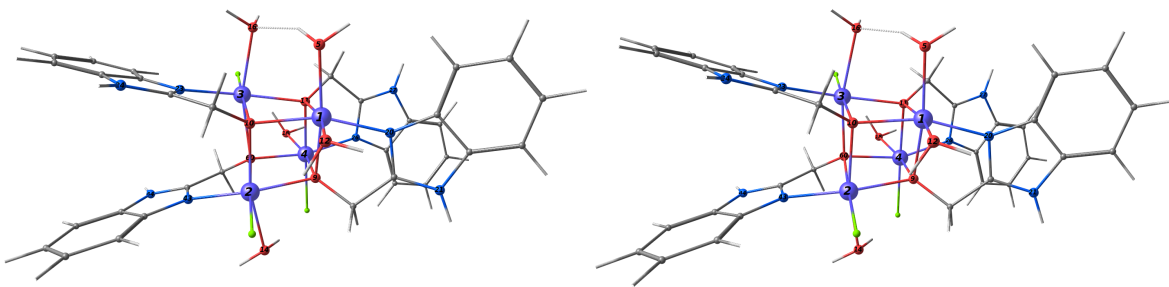


Figure S50. DFT-optimized structures of oxidized (left) vs reduced (right) forms of water-substituted complex **1**.

Table S17. Selected metrical parameters for the oxidized and reduced forms of complex **1**.

Oxidized		Reduced	
Bond	Distances (Å)	Bond	Distances (Å)
Ni1 – O5	2.087	Ni1 – O5	2.120
Ni1 – O9	2.069	Ni1 – O9	2.074
Ni1 – O10	2.077	Ni1 – O10	2.078
Ni1 – O11	2.140	Ni1 – O11	2.111
Ni1 – O12	2.117	Ni1 – O12	2.146
Ni1 – N20	2.042	Ni1 – N20	2.051

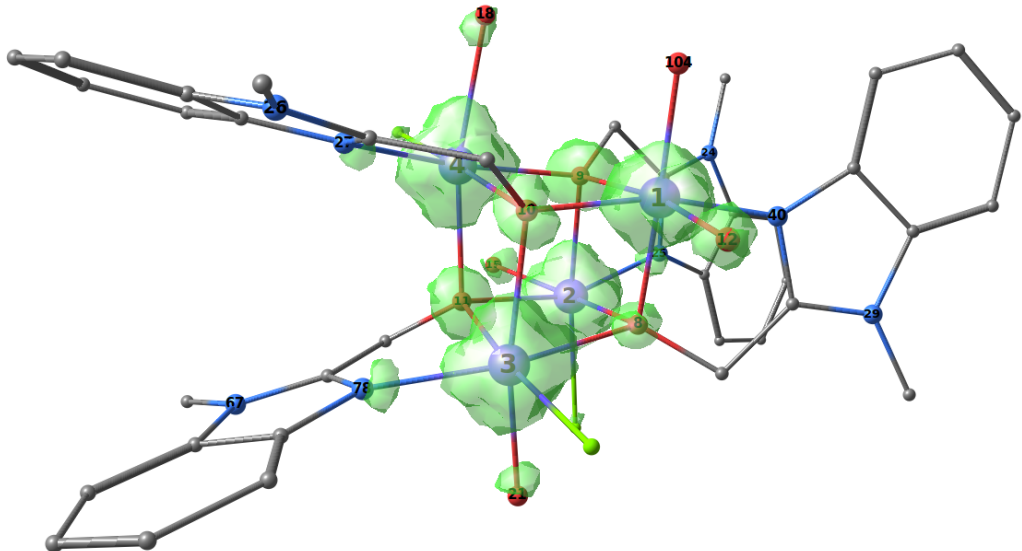


Figure S51. Spin density plot for water-substituted complex **1** upon successive oxidation and deprotonation of the Ni₁ center.
Hydrogen atoms are omitted for clarity.

Table S18. Mulliken spin populations for optimized complex **1** upon successive oxidation and deprotonation.

Spin populations	
Ni1	0.81
Ni2	1.55
Ni3	1.53
Ni4	1.54
Ci5	0.09
Ci6	0.10
Ci7	0.10
O8	0.09
O9	0.24
O10	0.14
O11	0.23
O12	0.08
O15	0.06
O18	0.05
O21	0.06
O104	-0.02
N25	0.07
N27	0.07
N40	0.03
N78	0.08

Table S19. Free Gibbs enthalpies (Eh) in the initial (reduced) and oxidized forms of **1**.

Complex 1 with 2 H ₂ O in Ni ₁	
Gibbs free energy S=9 (Eh)	-9773.33278032
Gibbs free energy S=8 (Eh)	-9773.13224504

The value matching best the experiment is obtained when considering the initial (“reduced” form in Figure S52) complex **1** with two water molecules coordinated to Ni₁ and the oxidized form. The redox process is metal based, with the Ni(II)/Ni(III) couple considered for the redox potential calculation.

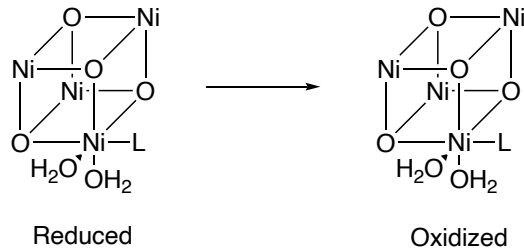


Figure S52. Redox couple to calculate the theoretical redox potential.

Table S20. Calculated vs experimental redox potential for **1**.

Δ Free Gibbs energy (Eh)	0.20010574
Δ Free Gibbs energy (V)	5.4451573335
vs SHE (V)	4.281
E(vs. RHE) calculated (V)	1.164
E(vs. RHE) experimental (V)	1.810

I2M MECHANISM

After the oxidation of **1**, deprotonation of a water molecule is expected to form a hydroxy group that may attack a second water molecule (coordinated at an adjacent Ni center) to form an O-O bond. The results of our calculations support that the deprotonation event is likely to occur upon oxidation (Table S21).

Deprotonation with acid/base couple: $(\text{H}_2\text{PO}_4)^{-}/(\text{HPO}_4^{2-})$

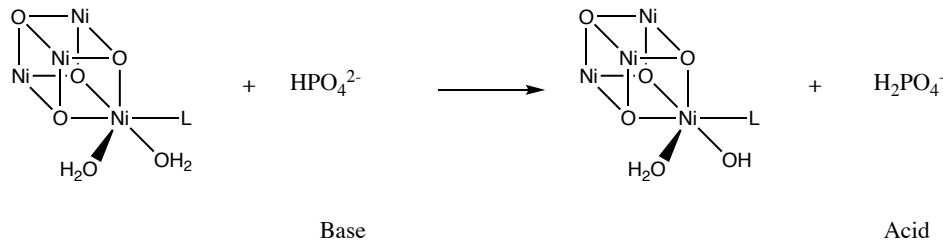


Figure S53. Deprotonation of a H_2O molecule of **1** in water.

Inorganic phosphate near physiological (neutral) pH primarily consists of a mixture of HPO_4^{2-} and H_2PO_4^- ions.

- **OXIDIZED COMPLEX**

Table S21. Oxidized **1** deprotonation at Ni_1 with $(\text{H}_2\text{PO}_4)^{-}/(\text{HPO}_4^{2-})$ acid/base couple.

Free Gibbs energy (Eh)	
Complex 1 with OH^- in Ni_1 (ox.)	-9772.715248
Acid $((\text{H}_2\text{PO}_4)^{-})$	-643.9620359
Complex 1 with OH^- (ox.) + acid	-10416.67728
Complex 1 with 2 H_2O in Ni_1 (ox.)	-9773.132675
Base $((\text{HPO}_4)^{2-})$	-643.4944304
Complex 1 with 2 H_2O in Ni_1 (ox.) + base	-10416.6271
Δ Free Gibbs energy (Eh) ((Complex 1 + acid) – (Complex 1 + base))	-0.05017923
Δ Free Gibbs energy (kcal.mol ⁻¹)	-31.5

2. $[(\mu_3\text{-}1\text{-methyl}\text{-}2\text{-benzimidazole}\text{-}\text{CH}_2\text{O})\text{NiCl}(\text{H}_2\text{O})]_4$ complex 2

FULL STRUCTURE OPTIMIZATION OF 2 IN WATER

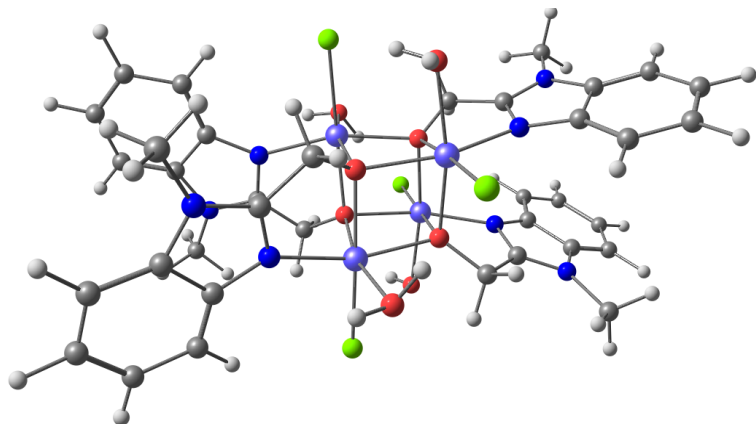
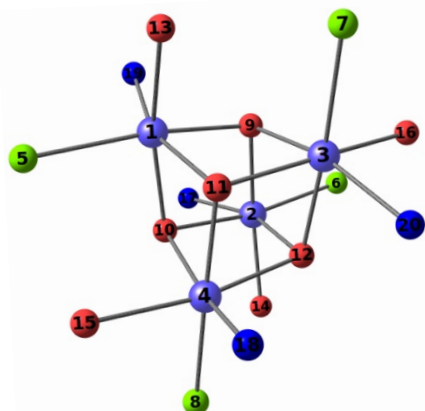


Figure S54. Optimized structure of complex **2** in water.

The standard deviations are in the range of the DFT precision, being 0.035 Å and 1.5 ° for bond lengths and angles, respectively.

Table S22. Bond length difference between experimental and calculated **2** in water.

	exptl	calcd	Δ	$(\text{calcd}-\text{exptl})^2$
Ni1O9	2.0780	2.096	0.018	0.0003240
Ni1O10	2.1010	2.129	0.028	0.0007840
Ni1O11	2.0580	2.091	0.033	0.0010890
Ni1O13	2.1180	2.163	0.045	0.0020250
Ni1Cl5	2.3860	2.405	0.019	0.0003610
Ni1N19	2.0110	2.053	0.042	0.0017640
Ni2O9	2.1040	2.126	0.022	0.0004840
Ni2O10	2.0830	2.096	0.013	0.0001690
Ni2O12	2.0670	2.096	0.029	0.0008410
Ni2O14	2.1230	2.162	0.039	0.0015210
Ni2Cl6	2.3650	2.401	0.036	0.0012960
Ni2N17	2.0330	2.056	0.023	0.0005290
Ni3O9	2.0400	2.099	0.059	0.0034810
Ni3O11	2.1230	2.122	-0.001	0.0000010
Ni3O12	2.0910	2.086	-0.005	0.0000250
Ni3O16	2.1070	2.173	0.066	0.0043560
Ni3Cl7	2.3800	2.409	0.029	0.0008410
Ni3N20	2.0290	2.046	0.017	0.0002890
Ni4O10	2.0450	2.101	0.056	0.0031360
Ni4O11	2.0760	2.088	0.012	0.0001440
Ni4O12	2.1020	2.124	0.022	0.0004840
Ni4O15	2.1090	2.169	0.060	0.0036000
Ni4Cl8	2.3830	2.411	0.028	0.0007840
Ni4N18	2.0370	2.046	0.009	0.0000810



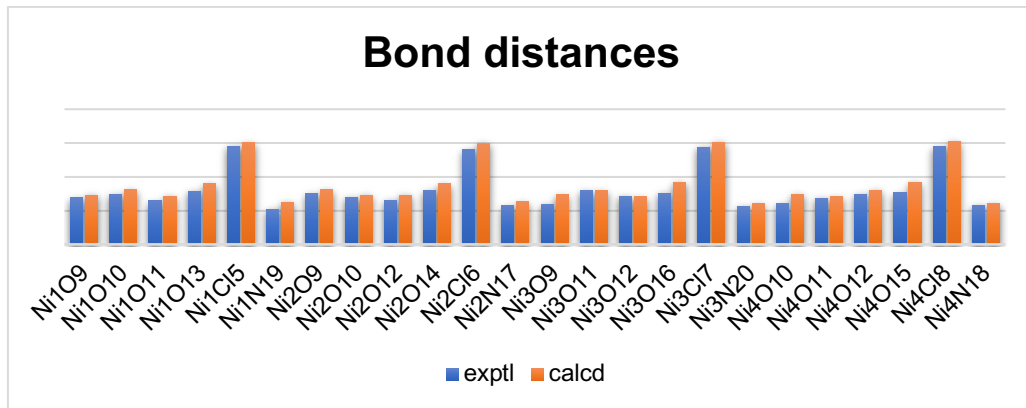


Figure S55. Distances around Ni(II) for the optimized **2** in water.

Table S23. Angle difference between experimental and calculated **2** in water.

	exptl	calcd	Δ°	$(\text{calcd}-\text{exptl})^2$		exptl	calcd	Δ°	$(\text{calcd}-\text{exptl})^2$
O9Ni1O10	79.70	78.80	-0.90	0.81	O9Ni3O11	81.60	81.00	-0.60	0.36
O9Ni1O11	82.20	81.80	-0.40	0.16	O9Ni3O12	82.50	82.10	-0.40	0.16
O9Ni1O13	95.50	95.90	0.40	0.16	O9Ni3O16	91.00	89.20	-1.80	3.24
O9Ni1N19	80.40	80.00	-0.40	0.16	O9Ni3N20	159.60	161.20	1.60	2.56
O9Ni1C15	17.,80	173.20	-0.60	0.36	O9Ni3Cl7	96.70	96.00	-0.70	0.49
O10Ni1O11	81.00	81.70	0.70	0.49	O11Ni3O12	79.00	79.50	0.50	0.25
O10Ni1O13	167.00	166.60	-0.40	0.16	O11Ni3O16	169.90	169.40	-0.50	0.25
O10Ni1N19	99.40	102.40	3.00	9.00	O11Ni3N20	97.30	101.70	4.40	19.36
O10Ni1C15	94.30	94.40	0.10	0.01	O11Ni3Cl7	98.60	97.10	-1.50	2.25
O11Ni1O13	86.40	85.90	-0.50	025	O12Ni3O16	93.40	95.30	1.90	3.61
O11Ni1N19	162.30	160.30	-2.00	4.00	O12Ni3N20	77.30	80.10	2.80	7.84
O11Ni1C15	98.60	97.80	-0.80	0.64	O12Ni3Cl7	177.60	176.30	-1.30	1.69
O13Ni1N19	91.60	88.70	-2.90	8.41	O16Ni3N20	87.30	86.40	-0.90	0.81
O13Ni1C15	90.70	90.80	0.10	0.01	O16Ni3Cl7	88.90	87.80	-1.10	1.21
N19Ni1C15	99.10	101.20	2.10	4.41	N20Ni3Cl7	103.60	102.10	-1.50	2.25
O9Ni2O10	79.50	78.90	-0.60	0.36	O10Ni4O11	81.90	81.90	0.00	0.00
O9Ni2O12	81.60	81.20	-0.40	0.16	O10Ni4O12	81.40	80.90	-0.50	0.25
O9Ni2O14	168.20	166.40	-1.80	3.24	O10Ni4O15	88.50	88.80	0.30	0.09
O9Ni2N17	99.80	102.70	2.90	8.41	O10Ni4N18	161.20	161.00	-0.20	0.04
O9Ni2C16	94.70	94.30	-0.40	0.16	O10Ni4Cl8	99.40	96.00	-3.40	11.56
O10Ni2O12	81.40	81.70	0.30	0.09	O11Ni4O12	79.80	79.50	-0.30	0.09
O10Ni2O14	94.40	95.90	1.50	2.25	O11Ni4O15	94.40	95.80	1.40	1.96
O10Ni2N17	80.00	79.90	-0.10	0.01	O11Ni4N18	80.20	80.20	0.00	0.00
O10Ni2C16	174.20	173.20	-1.00	1.00	O11Ni4Cl8	175.40	176.00	0.60	0.36
O12Ni2O14	87.50	85.60	-1.90	3.61	O12Ni4O15	168.90	169.20	0.30	0.09
O12Ni2N17	160.80	160.00	-0.80	0.64	O12Ni4N18	101.20	101.90	0.70	0.49
O12Ni2C16	98.40	98.30	-0.10	0.01	O12Ni4Cl8	96.00	96.90	0.90	0.81
O14Ni2N17	89.00	88.50	-0.50	0.25	O15Ni4N18	87.00	86.70	-0.30	0.09
O14Ni2C16	91.40	90.90	-0.50	0.25	O15Ni4Cl8	90.00	87.50	-2.50	6.25
N17Ni2C16	100.50	100.90	0.40	0.16	N18Ni4Cl8	98.80	102.30	3.50	12.25

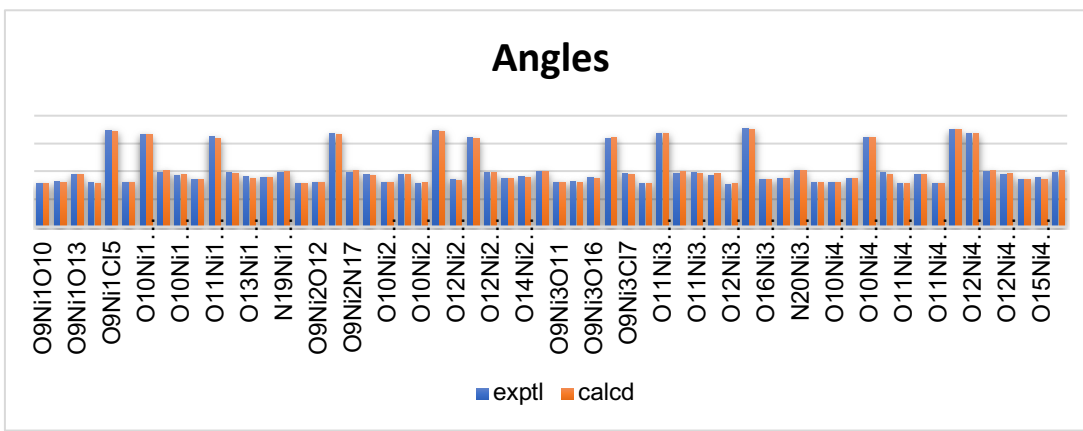


Figure S56. Angles around Ni(II) for the optimized **2** in water.

SPIN DENSITY PLOTS

From Mulliken spin population analysis, we observe that 92% of the spin density is found at the Ni(II) metal centers as expected in the case of a tetranuclear complex with four high spin Ni(II) ions ($S = 1$ each).

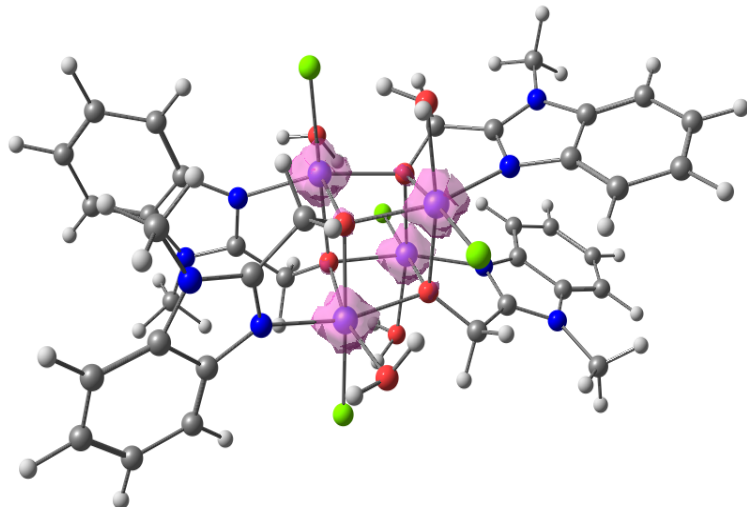


Figure S57. Spin density of optimized **2** in water.

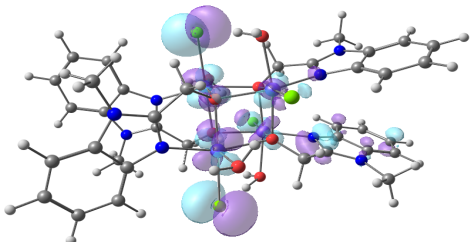
Table S24. Mulliken atomic charges and spin population for **2** in water.

Atom	Spin population
Ni	1.546341
Ni	1.546332
Ni	1.536881
Ni	1.537462
Cl	0.088120
Cl	0.088402
Cl	0.084466
Cl	0.084619
O	0.213937
O	0.213954
O	0.217559
O	0.217482

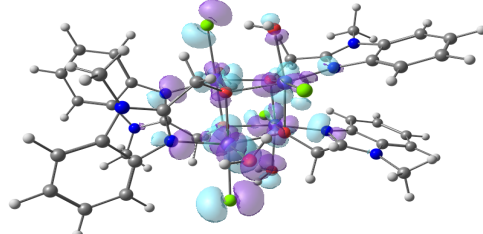
SINGLY OCCUPIED MOLECULAR ORBITALS

The singly occupied molecular orbitals are mainly metal based and consistent with the description of a tetranuclear complex with 4 high spin Ni(II) centers.

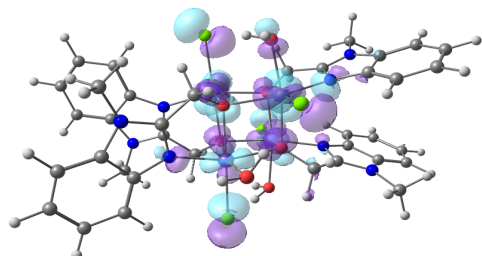
-5.5951eV



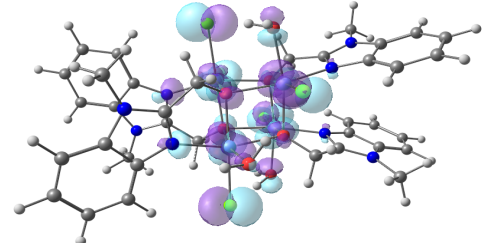
-5.5634eV



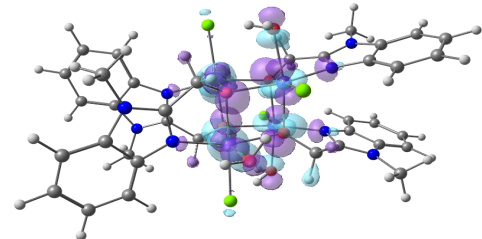
-5.5144 eV



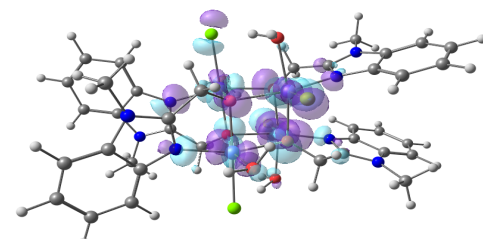
-5.0118 eV



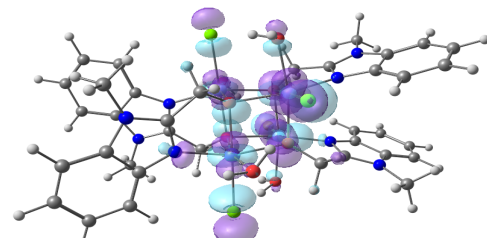
-4.9414 eV



-4.8872 eV



-4.8703 eV



-4.8529 eV

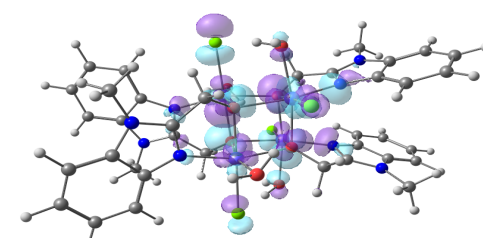


Figure S58. Singly occupied molecular orbitals of **2** in water.

MAGNETIC PROPERTIES

Broken symmetry

The ferromagnetic behavior of complex **2** can be rationalized by examining the value of the angles Ni-O-Ni that are overall lower than 99°.

Table S25. Calculated exchange coupling constants J , and Ni-O-Ni angles for **2** in water.

	Energies (Eh)	ΔE (Eh)	ΔE (cm^{-1})		Eh	cm^{-1}
$\alpha\alpha\alpha\alpha$	-10312.115255	0.000000	0			
$\alpha\alpha\alpha\beta$	-10312.115054	0.000201	44	J1 – AB	0.00000925	2.03
$\alpha\alpha\beta\alpha$	-10312.115036	0.000219	48	J2 – AC	0.000013125	2.88
$\alpha\beta\alpha\alpha$	-10312.115116	0.000139	31	J3 – AD	0.000013375	2.94
$\beta\alpha\alpha\alpha$	-10312.115112	0.000143	31	J4 – BC	0.000018125	3.98
$\alpha\beta\beta\alpha$	-10312.115042	0.000213	47	J5 – BD	0.000013375	2.94
$\alpha\beta\alpha\beta$	-10312.114998	0.000257	56	J6 – CD	0.000007375	1.62
$\alpha\alpha\beta\beta$	-10312.115047	0.000208	46			

Angles	
Ni1O6Ni4	96.9
Ni1O7Ni4	98.2
Ni1O5Ni3	97.9
Ni1O7Ni3	97.4
Ni1O5Ni2	100.9
Ni1O6Ni2	100.8
Ni2O5Ni3	96.9
Ni2O8Ni3	97.9
Ni2O8Ni4	97.4
Ni2O6Ni4	98.1
Ni3O8Ni4	100.2
Ni3O7Ni4	100.3

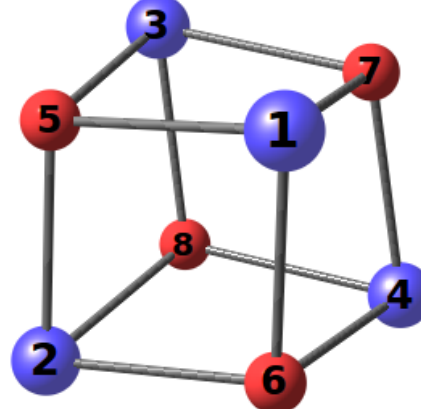


Table S26. Spin ladder of the optimized **2** in water.

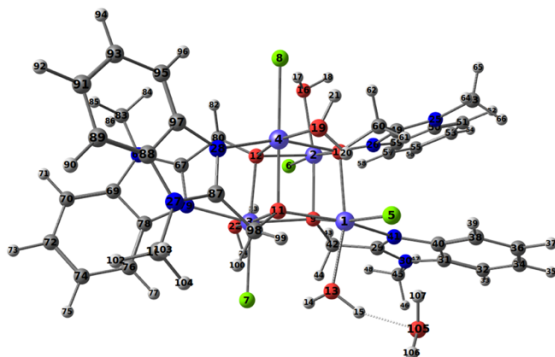
Spin states	Energy (cm^{-1})
S = 4	0
S = 3	18.6
S = 3	20.6
S = 2	26.3
S = 3	32.7
S = 2	34.5

LIGAND EXCHANGE

1. Relaxed surface scan

We investigated the dissociation of a Cl⁻ (center 5) from a Ni center (center 1) and the formation of a bond between the metal and an external water molecule (centers 105, 106, 107). We conducted a relaxed scan surface, which consists in a full geometry optimization at each step while keeping constrained the distance between the Ni and the water (fixed value for the Ni₁-O₁₀₅ bond). Following the energy profile for the 10 optimizations steps, it is possible to observe the dissociation of the Cl⁻ upon coordination of the H₂O molecule to the Ni center (Figure S59).

A)



B)

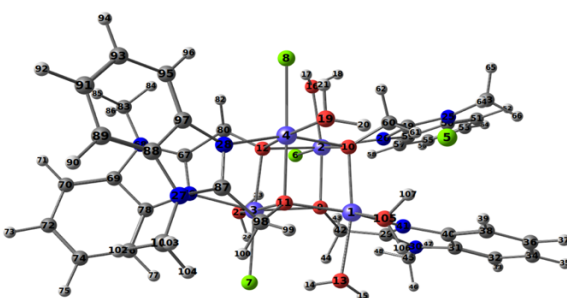


Figure S59. Relaxed surface scan: A) Ni₁-H₂O distance = 3.86 Å, B) Ni₁-H₂O distance = 2.10 Å.

Table S27. Relaxed surface scan of bond length between atoms 1 (Ni₁) and 105 (O) from 3.86 Å to 2.10 Å in 10 steps.

Bond length (Å)	Energy (Eh)
3.83	-10391.65940484
3.67	-10391.65873435
3.47	-10391.65630586
3.27	-10391.65339793
3.08	-10391.64773923
2.88	-10391.63954228
2.69	-10391.62809169
2.49	-10391.65092787
2.30	-10391.65462411
2.10	-10391.65679310

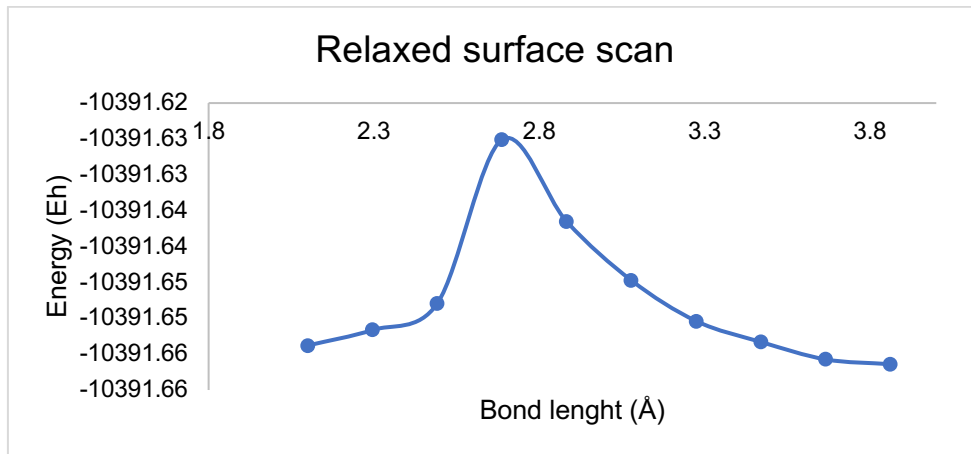


Figure S60. Relaxed surface scan of **2** for bond distance between Ni₁ and H₂O.

Numerical frequency calculations were performed using both the initial and final steps of the relaxed surface scan, for which the H₂O molecule is at 3.86 Å and 2.10 Å from the Ni center respectively. A Gibbs free energy difference of 1.6 kcal mol⁻¹ was obtained, supporting the feasibility of the ligand exchange process (Table S28).

Table S28. Gibbs free energy ligand exchange for **2** in water.

Free Gibbs energy (Eh)	
Complex 2 with H ₂ O at 2.10 Å	-10390.96414
Complex 2 with H ₂ O at 3.86 Å	-10390.96675
Δ Free Gibbs energy (Eh)	0.00260837
Δ Free Gibbs energy (kcal.mol ⁻¹)	1.6

OXIDATION

Table S29. Free Gibbs enthalpies (Eh) in the reduced and oxidized forms of 2.

	2 without Cl in Ni ₁	2 with 2 H ₂ O in Ni ₁	H ₂ O	Cl
Gibbs free energy S=9 (Eh)	-9854.037775	-9930.51218	-76.4731172	-460.432199
Gibbs free energy S=8 (Eh)	-9853.833656	-9930.311287	-76.4731172	-460.432199

After computing all possible combinations for the redox potential, the value matching best the experiment is obtained when considering the reduced complex **2** with two water molecules coordinated to Ni_i and the oxidized complex **2** without a water molecule coordinated to Ni_i. The redox process is metal based, with the Ni(II)/Ni(III) couple considered to calculate the potential. This result is consistent first with the exchange of Cl⁻ for H₂O in the initial (“reduced” in Figure S61) form of the complex. Upon oxidation, a coordinated molecule of H₂O can be initially deprotonated and ultimately oxidized to O₂.

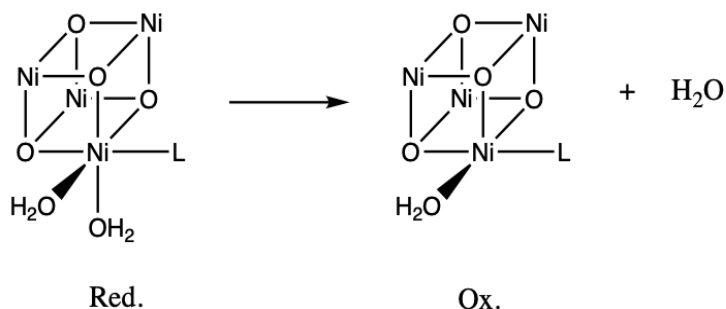


Figure S61. Redox couple to calculate the theoretical redox potential.

Table S30. Calculated vs experimental redox potential for complex 2.

Δ Free Gibbs energy (Eh)	0.20540717
Δ Free Gibbs energy (V)	5.58941667
vs SHE (V)	4.281
E(vs. RHE) calculated (V)	1.308
E(vs. RHE) experimental (V)	1.711

I2M MECHANISM

After the oxidation of **2**, deprotonation of a water molecule is expected to form a hydroxyl ligand that may attack a second water molecule (coordinated to an adjacent Ni center) to form an O-O bond. The results of our calculations support that the deprotonation event is much more likely to occur upon oxidation (Tables S31 and S32).

Deprotonation with acid/base couple: $(\text{H}_2\text{PO}_4)^{-}/(\text{HPO}_4)^{2-}$

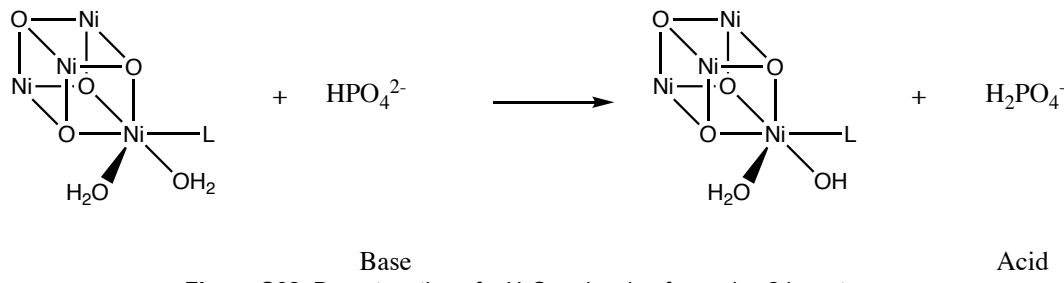


Figure S62. Deprotonation of a H_2O molecule of complex **2** in water.

Inorganic phosphate near physiological (neutral) pH primarily consists of a mixture of HPO_4^{2-} and H_2PO_4^- ions, which can act as bases.

- INITIAL COMPLEX

Table S31. Deprotonation of **2** at Ni_1 with $(\text{H}_2\text{PO}_4)^{-}/(\text{HPO}_4)^{2-}$ acid/base couple.

Free Gibbs energy (Eh)	
Complex 2 with OH^- in Ni_1 (red.)	-9930.04541
Acid $((\text{H}_2\text{PO}_4)^{-})$	-643.9620359
Complex 2 with OH^- (red.) + acid	-10574.00745
Complex 2 with 2 H_2O in Ni_1 (red.)	-9930.51218
Base $((\text{HPO}_4)^{2-})$	-643.4944304
Complex 2 with 2 H_2O in Ni_1 (red.) + base	-10574.00661
Δ Free Gibbs energy (Eh) $((\text{Complex } \mathbf{2} + \text{acid}) - (\text{Complex } \mathbf{2} + \text{base}))$	-0.00083527
Δ Free Gibbs energy (kcal.mol⁻¹)	-0.5

- OXIDIZED COMPLEX

Table S32. Oxidized **2** deprotonation with $(\text{H}_2\text{PO}_4)^{-}/(\text{HPO}_4)^{2-}$ acid/base couple.

	Free Gibbs energy (Eh)
Complex 2 with OH^- in Ni_1 (ox.)	-9929.869377
Acid $((\text{H}_2\text{PO}_4)^{-})$	-643.9620359
Complex 2 with OH^- (ox.) + acid	-10573.83141
Complex 2 with 2 H_2O in Ni_1 (ox.)	-9930.311287
Base $((\text{HPO}_4)^{2-})$	-643.4944304
Complex 2 with 2 H_2O in Ni_1 (ox.) + base	-10573.80572
Δ Free Gibbs energy (Eh) ((Complex 2 + acid) – (Complex 2 + base))	-0.02569509
Δ Free Gibbs energy (kcal.mol⁻¹)	-16.1

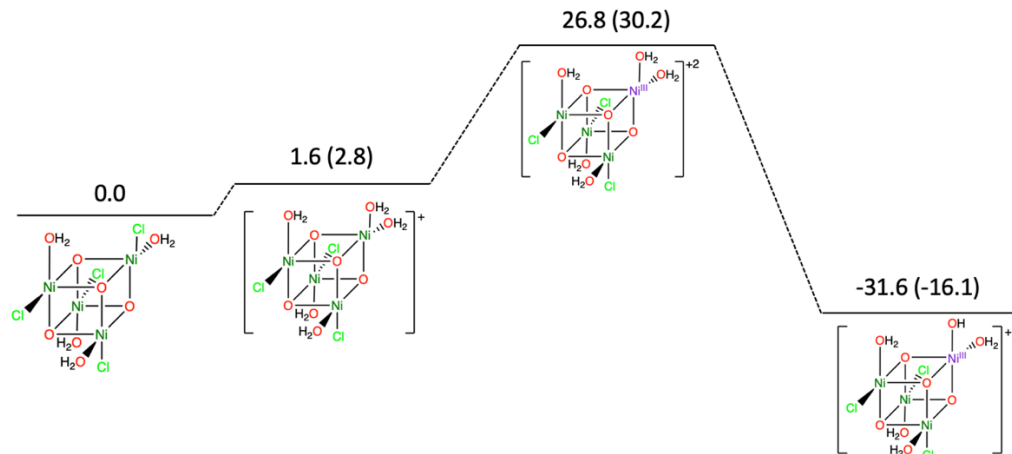


Figure S60. Calculated free energy changes (kcal mol⁻¹) for the proposed I2M mechanism leading to O-O bond formation from complexes **1** and **(2)**.

EPR PARAMETERS

Table S33. DFT-calculated EPR parameters for the one-electron oxidized complex **1**.

*Only hyperfine couplings for coordinated nitrogen atoms are considered.

g-tensor	g ₁	g ₂	g ₃	g _{iso}
Calculated	2.031	2.038	2.075	2.048
Simulated	2.045	2.053	2.061	2.053
A-tensor ¹⁴ N (MHz)	A ₁	A ₂	A ₃	A _{iso}
Calculated*	30.3	31.5	40.6	34.1
	15.5	17.8	24.4	19.2
	10.9	13.0	18.1	14.0
	30.0	31.6	40.9	34.1
Simulated	-	-	-	25

CARTESIAN COORDINATES

Optimized structures for complex **1**

Initial structure

Ni	9.086556	16.067862	9.195735
Ni	8.210869	16.949936	6.284416
Ni	6.327736	15.014511	8.081173
Ni	6.577672	18.104514	8.724844
Cl	9.363937	14.064999	10.492788
Cl	10.489796	16.937988	5.520370
Cl	4.027823	14.986874	8.783312
Cl	6.356804	20.227056	7.616242
O	8.605231	17.827489	8.148625
O	8.320818	15.187654	7.462675
O	7.013657	16.255043	9.628702
O	11.035097	15.789130	8.295640
H	10.969223	16.189446	7.379176
O	8.023974	18.933650	5.430057
H	8.941567	19.266022	5.404452
O	6.651993	13.291805	9.356017
H	7.503089	13.482673	9.850965
O	4.436194	18.003901	9.014503
H	4.208286	17.027975	9.004496
N	9.926057	17.464601	10.449525
N	10.722385	19.541698	10.600814
H	10.937058	20.498688	10.334879
N	6.319974	13.690547	6.516649

N	7.585263	12.319504	5.296915
H	8.421281	11.888305	4.912918
N	6.760185	18.701965	10.683900
N	6.685283	18.041936	12.812327
H	6.633756	17.417597	13.612433
C	10.051956	18.639752	9.835552
C	10.554614	17.599167	11.685870
C	10.733039	16.686861	12.734165
H	10.347412	15.670217	12.653529
C	11.423897	17.128734	13.863339
H	11.581744	16.441197	14.695816
C	11.926529	18.444298	13.956409
H	12.461146	18.749013	14.857324
C	11.756771	19.365537	12.921062
H	12.144548	20.382348	12.989709
C	11.066439	18.918745	11.791984
C	9.526806	18.858835	8.448257
H	9.050813	19.852395	8.369860
H	10.373715	18.838265	7.734322
N	7.200877	16.281772	4.630883
N	5.225471	16.266646	3.598472
H	4.225316	16.378599	3.458554
C	5.898416	16.521230	4.753581
C	7.400548	15.854185	3.322005
C	8.566167	15.475518	2.643012
H	9.531847	15.494324	3.148942
C	8.439559	15.090873	1.307324
H	9.329437	14.793010	0.750445
C	7.187501	15.078928	0.655849
H	7.132730	14.772092	-0.389697
C	6.016476	15.453423	1.318105
H	5.048140	15.446565	0.816761
C	6.147895	15.839661	2.654009
C	5.314497	17.049710	6.030734
H	5.075466	18.123234	5.905219
H	4.371616	16.526340	6.268552
O	6.267700	16.877391	7.063257
C	7.562488	13.335133	6.202404
C	5.476652	12.859407	5.786156
C	4.078780	12.781837	5.731810
H	3.463766	13.446858	6.338753
C	3.517359	11.821834	4.888494
H	2.431409	11.734737	4.826475
C	4.319774	10.957049	4.113602
H	3.840495	10.220268	3.467265
C	5.714114	11.020842	4.156695
H	6.336440	10.353039	3.560174
C	6.271933	11.981416	5.003601
C	8.751301	13.990331	6.841761
H	9.184965	13.303580	7.593864

H	9.532510	14.192035	6.087832
C	6.699170	17.657638	11.508028
C	6.781278	19.837492	11.491228
C	6.836257	21.198982	11.165589
H	6.868698	21.515608	10.122796
C	6.838923	22.114490	12.218879
H	6.878561	23.182417	11.998406
C	6.790202	21.694168	13.565386
H	6.793499	22.443112	14.358710
C	6.736373	20.341259	13.906512
H	6.698278	20.013901	14.945900
C	6.732319	19.428366	12.849313
C	6.621658	16.253145	10.988464
H	7.268579	15.586657	11.586260
H	5.581352	15.886045	11.090512
H	11.714269	16.313606	8.758662
H	7.549133	19.480426	6.123953
H	5.935812	13.348266	10.017039
H	4.191129	18.317598	9.904598

Structure upon ligand exchange

Ni	8.443994	9.579132	10.355146
Ni	7.802874	11.425619	12.811273
Ni	5.441291	10.294453	10.880114
Ni	6.877626	8.399677	12.947242
O	7.933049	9.643136	8.300982
Cl	9.785941	12.701852	12.383435
Cl	3.381759	9.102552	11.059652
Cl	7.348186	8.32577	15.291979
O	8.612644	9.533819	12.422842
O	7.284093	11.259724	10.745291
O	6.649034	8.585319	10.852148
O	10.044772	10.940038	9.925518
H	10.07925	11.568885	10.708286
O	8.415458	11.123738	14.845216
H	8.055755	10.22397	15.108626
O	5.235615	9.958438	8.63298
H	4.529608	9.279809	8.634664
O	4.877024	7.670437	13.318893
H	4.300192	8.031447	12.58609
N	9.828925	8.077882	10.528409
N	11.389103	7.208176	11.861715
H	11.948574	7.053779	12.696032
N	4.797755	12.20284	10.563177
N	5.345378	14.224366	9.80275
H	5.919726	14.980412	9.440163
N	7.425001	6.514703	12.371394
N	7.275731	4.972882	10.768643
H	7.052859	4.553632	9.870072
C	10.36785	8.096329	11.748563

C	10.542453	7.128372	9.79897
C	10.419987	6.698431	8.471465
H	9.661244	7.112918	7.807094
C	11.306181	5.718373	8.023256
H	11.236257	5.36678	6.992971
C	12.293117	5.171681	8.870645
H	12.967014	4.407873	8.480383
C	12.428195	5.586724	10.196548
H	13.190361	5.166605	10.853267
C	11.53997	6.569314	10.639172
C	9.884942	9.043275	12.807779
H	9.834536	8.535629	13.786724
H	10.603603	9.879951	12.903077
N	6.495984	12.869929	13.456814
N	4.552569	13.266311	14.474377
H	3.645369	13.083834	14.894919
C	5.369873	12.331368	13.922508
C	6.416904	14.235608	13.722933
C	7.312985	15.279866	13.459086
H	8.265324	15.080888	12.966846
C	6.940345	16.564429	13.857017
H	7.616881	17.399398	13.66813
C	5.708883	16.812556	14.500713
H	5.456773	17.832335	14.795247
C	4.805441	15.783036	14.770901
H	3.853649	15.97161	15.268255
C	5.18269	14.498577	14.372061
C	5.115732	10.854859	13.843418
H	5.281549	10.398313	14.837828
H	4.066838	10.659218	13.560964
O	6.014487	10.298824	12.898725
C	5.786998	12.981194	10.126037
C	3.63898	12.976364	10.51991
C	2.313836	12.67284	10.857831
H	2.048196	11.680843	11.223936
C	1.361506	13.679907	10.696227
H	0.319718	13.474962	10.947602
C	1.711151	14.959369	10.213597
H	0.934803	15.717572	10.101528
C	3.027416	15.27752	9.874074
H	3.300254	16.265244	9.501606
C	3.977342	14.266244	10.035571
C	7.1884	12.461826	9.997753
H	7.413599	12.280608	8.930015
H	7.914343	13.208911	10.362957
C	7.035709	6.26271	11.123452
C	7.946135	5.321883	12.868762
C	8.493032	5.005329	14.119189
H	8.558843	5.76318	14.900388
C	8.932737	3.696158	14.316475

H	9.361298	3.415979	15.280036
C	8.836776	2.721178	13.30005
H	9.193023	1.708925	13.496692
C	8.295703	3.021253	12.048604
H	8.220592	2.270135	11.261911
C	7.854443	4.332513	11.855805
C	6.379596	7.316847	10.281144
H	6.74217	7.25194	9.240502
H	5.287556	7.134568	10.258694
H	10.913376	10.496996	9.911087
H	7.988015	11.762667	15.445011
H	4.839987	10.722843	8.171122
H	4.822323	6.699995	13.241054
H	8.25979	8.959034	7.690374
H	6.942869	9.631461	8.231022

Structure upon one-electron oxidation

Ni	8.425523	9.570599	10.358066
Ni	7.777466	11.361447	12.85
Ni	5.41165	10.321587	10.828782
Ni	6.793907	8.366038	12.898466
O	7.936268	9.653041	8.330569
Cl	9.678842	12.585405	12.491312
Cl	3.368618	9.193416	11.082402
Cl	7.226376	8.237234	15.176217
O	8.578431	9.517246	12.420619
O	7.266784	11.245301	10.764152
O	6.5939	8.593425	10.878912
O	10.01504	10.909248	9.951584
H	10.083591	11.515679	10.742143
O	8.403972	11.021435	14.873282
H	8.020675	10.14362	15.159004
O	5.23733	10.00408	8.660193
H	4.529563	9.333857	8.56413
O	4.825257	7.688543	13.251645
H	4.224778	8.034758	12.525965
N	9.78259	8.055303	10.538038
N	11.359482	7.200393	11.85983
H	11.931096	7.055102	12.688042
N	4.81355	12.237435	10.575792
N	5.398	14.25659	9.84253
H	5.985283	15.007277	9.488548
N	7.366609	6.573684	12.366555
N	7.31172	5.02437	10.77612
H	7.112613	4.582862	9.881847
C	10.334941	8.08123	11.752958
C	10.492093	7.104451	9.804682
C	10.352525	6.660932	8.483532
H	9.580841	7.059823	7.824944
C	11.237123	5.680682	8.034619

H	11.154297	5.317405	7.009574
C	12.237577	5.146795	8.874531
H	12.909253	4.381919	8.482907
C	12.387492	5.573509	10.194356
H	13.157691	5.161854	10.846664
C	11.500328	6.556394	10.638231
C	9.851794	9.018597	12.819237
H	9.783338	8.50648	13.793057
H	10.563807	9.856209	12.932199
N	6.510811	12.763643	13.481768
N	4.55195	13.162453	14.459185
H	3.646238	12.98426	14.885977
C	5.384623	12.222201	13.958299
C	6.41204	14.139337	13.685609
C	7.290863	15.190179	13.393254
H	8.25114	14.997705	12.916048
C	6.888482	16.478123	13.74398
H	7.550386	17.318612	13.531207
C	5.647071	16.724031	14.369169
H	5.373195	17.747986	14.626243
C	4.761887	15.688339	14.666448
H	3.802313	15.872355	15.1496
C	5.166192	14.399143	14.312856
C	5.171541	10.745017	13.915572
H	5.369433	10.291964	14.901989
H	4.141645	10.495073	13.617698
O	6.110036	10.2382	12.949168
C	5.817902	13.005696	10.150016
C	3.665145	13.028959	10.538144
C	2.333519	12.745024	10.866789
H	2.045622	11.755321	11.22076
C	1.401923	13.771725	10.712772
H	0.355601	13.583076	10.957156
C	1.777154	15.050159	10.247044
H	1.015293	15.823555	10.141068
C	3.099665	15.348311	9.917232
H	3.393617	16.334611	9.557916
C	4.029371	14.317476	10.07084
C	7.207438	12.459761	10.02228
H	7.438488	12.270565	8.958724
H	7.950655	13.183331	10.3956
C	6.996841	6.29354	11.110575
C	7.96092	5.421234	12.884119
C	8.526075	5.134335	14.13325
H	8.557182	5.889735	14.916798
C	9.033916	3.850579	14.327746
H	9.479125	3.596406	15.290519
C	8.986474	2.870207	13.313957
H	9.394742	1.878267	13.510921
C	8.429105	3.141288	12.065216

H	8.388974	2.389912	11.276635
C	7.922744	4.428014	11.871416
C	6.31105	7.327338	10.280344
H	6.662269	7.296493	9.236752
H	5.221011	7.14493	10.27214
H	10.886691	10.477104	9.876693
H	8.05445	11.683289	15.499121
H	4.896109	10.787423	8.184604
H	4.741195	6.716455	13.237955
H	8.331789	9.052223	7.674776
H	6.955798	9.628483	8.19322

Structure upon deprotonation

Ni	8.439025	9.606909	10.447434
Ni	7.775064	11.449874	12.871393
Ni	5.436705	10.23998	10.859807
Ni	6.856482	8.369176	12.999909
O	8.014078	9.471373	8.635628
Cl	9.722758	12.754975	12.427202
Cl	3.397729	9.079214	11.113935
Cl	7.402329	8.336519	15.300169
O	8.643411	9.58589	12.372636
O	7.306447	11.188885	10.778767
O	6.657555	8.542527	10.941028
O	10.036244	11.031265	9.962161
H	10.076052	11.654763	10.750556
O	8.403589	11.139199	14.856396
H	8.047505	10.246661	15.152503
O	5.464512	10.033271	8.721249
H	4.935091	9.253943	8.471193
O	4.89516	7.647702	13.359931
H	4.314462	8.007623	12.625558
N	9.74926	8.188103	10.52151
N	11.332273	7.207476	11.725784
H	11.936446	6.995416	12.515965
N	4.838855	12.168273	10.568117
N	5.432184	14.139253	9.71381
H	6.023039	14.862992	9.313407
N	7.453511	6.489247	12.432215
N	7.328551	4.9386	10.835558
H	7.11759	4.514026	9.936416
C	10.357073	8.141416	11.713177
C	10.359091	7.23972	9.704717
C	10.136944	6.871268	8.372506
H	9.362176	7.361198	7.78444
C	10.949992	5.868784	7.844981
H	10.806892	5.557793	6.809337
C	11.955997	5.24637	8.614923
H	12.569062	4.467035	8.160773
C	12.187243	5.60521	9.942809

H	12.963652	5.12838	10.54103
C	11.373868	6.610038	10.470823
C	9.927892	9.0928	12.77773
H	9.844632	8.604321	13.761712
H	10.649327	9.924993	12.8628
N	6.444818	12.849249	13.494482
N	4.479662	13.21222	14.47703
H	3.570329	13.015772	14.886506
C	5.321744	12.290078	13.945801
C	6.33708	14.215685	13.749104
C	7.215837	15.276309	13.493999
H	8.179034	15.09623	13.016318
C	6.810451	16.554458	13.879536
H	7.472684	17.401964	13.696379
C	5.564061	16.780545	14.501879
H	5.286369	17.796438	14.786374
C	4.677613	15.734341	14.762301
H	3.713942	15.905295	15.242644
C	5.087502	14.456146	14.376458
C	5.101518	10.809311	13.869614
H	5.26573	10.361007	14.867746
H	4.061428	10.587934	13.574861
O	6.021769	10.27386	12.931535
C	5.839679	12.896798	10.081802
C	3.702968	12.970069	10.505615
C	2.373819	12.716259	10.868709
H	2.084871	11.747629	11.27711
C	1.447141	13.740842	10.6746
H	0.402947	13.574593	10.94378
C	1.825327	14.989669	10.135831
H	1.068056	15.763222	10.000697
C	3.145106	15.258055	9.769179
H	3.439685	16.221399	9.352185
C	4.06949	14.228857	9.962431
C	7.227067	12.34385	9.943384
H	7.411533	12.070468	8.89005
H	7.982283	13.089014	10.240714
C	7.089048	6.230408	11.176792
C	7.95572	5.294809	12.948738
C	8.474552	4.98064	14.211675
H	8.531525	5.739732	14.991911
C	8.901585	3.669588	14.423614
H	9.30849	3.391681	15.397027
C	8.820055	2.690333	13.410253
H	9.16542	1.676841	13.619013
C	8.307131	2.987728	12.146783
H	8.24316	2.234002	11.361721
C	7.879044	4.301015	11.939169
C	6.462821	7.285379	10.315366
H	6.899632	7.274045	9.302147

H	5.379423	7.084824	10.21079
H	10.919987	10.621843	9.90418
H	8.014357	11.797084	15.462199
H	6.445899	9.789728	8.560783
H	4.838052	6.676566	13.287921
H	8.596737	10.093943	8.159448

Optimized structures for complex 2

Initial structure

Ni	8.439025	9.606909	10.447434
Ni	7.775064	11.449874	12.871393
Ni	5.436705	10.23998	10.859807
Ni	6.856482	8.369176	12.999909
O	8.014078	9.471373	8.635628
Cl	9.722758	12.754975	12.427202
Cl	3.397729	9.079214	11.113935
Cl	7.402329	8.336519	15.300169
O	8.643411	9.58589	12.372636
O	7.306447	11.188885	10.778767
O	6.657555	8.542527	10.941028
O	10.036244	11.031265	9.962161
H	10.076052	11.654763	10.750556
O	8.403589	11.139199	14.856396
H	8.047505	10.246661	15.152503
O	5.464512	10.033271	8.721249
H	4.935091	9.253943	8.471193
O	4.89516	7.647702	13.359931
H	4.314462	8.007623	12.625558
N	9.74926	8.188103	10.52151
N	11.332273	7.207476	11.725784
H	11.936446	6.995416	12.515965
N	4.838855	12.168273	10.568117
N	5.432184	14.139253	9.71381
H	6.023039	14.862992	9.313407
N	7.453511	6.489247	12.432215
N	7.328551	4.9386	10.835558
H	7.11759	4.514026	9.936416
C	10.357073	8.141416	11.713177
C	10.359091	7.23972	9.704717
C	10.136944	6.871268	8.372506
H	9.362176	7.361198	7.78444
C	10.949992	5.868784	7.844981
H	10.806892	5.557793	6.809337
C	11.955997	5.24637	8.614923

H	12.569062	4.467035	8.160773
C	12.187243	5.60521	9.942809
H	12.963652	5.12838	10.54103
C	11.373868	6.610038	10.470823
C	9.927892	9.0928	12.77773
H	9.844632	8.604321	13.761712
H	10.649327	9.924993	12.8628
N	6.444818	12.849249	13.494482
N	4.479662	13.21222	14.47703
H	3.570329	13.015772	14.886506
C	5.321744	12.290078	13.945801
C	6.33708	14.215685	13.749104
C	7.215837	15.276309	13.493999
H	8.179034	15.09623	13.016318
C	6.810451	16.554458	13.879536
H	7.472684	17.401964	13.696379
C	5.564061	16.780545	14.501879
H	5.286369	17.796438	14.786374
C	4.677613	15.734341	14.762301
H	3.713942	15.905295	15.242644
C	5.087502	14.456146	14.376458
C	5.101518	10.809311	13.869614
H	5.26573	10.361007	14.867746
H	4.061428	10.587934	13.574861
O	6.021769	10.27386	12.931535
C	5.839679	12.896798	10.081802
C	3.702968	12.970069	10.505615
C	2.373819	12.716259	10.868709
H	2.084871	11.747629	11.27711
C	1.447141	13.740842	10.6746
H	0.402947	13.574593	10.94378
C	1.825327	14.989669	10.135831
H	1.068056	15.763222	10.000697
C	3.145106	15.258055	9.769179
H	3.439685	16.221399	9.352185
C	4.06949	14.228857	9.962431
C	7.227067	12.34385	9.943384
H	7.411533	12.070468	8.89005
H	7.982283	13.089014	10.240714
C	7.089048	6.230408	11.176792
C	7.95572	5.294809	12.948738
C	8.474552	4.98064	14.211675
H	8.531525	5.739732	14.991911
C	8.901585	3.669588	14.423614
H	9.30849	3.391681	15.397027
C	8.820055	2.690333	13.410253
H	9.16542	1.676841	13.619013
C	8.307131	2.987728	12.146783
H	8.24316	2.234002	11.361721
C	7.879044	4.301015	11.939169

C	6.462821	7.285379	10.315366
H	6.899632	7.274045	9.302147
H	5.379423	7.084824	10.21079
H	10.919987	10.621843	9.90418
H	8.014357	11.797084	15.462199
H	6.445899	9.789728	8.560783
H	4.838052	6.676566	13.287921
H	8.596737	10.093943	8.159448

Structure upon ligand exchange

Ni	3.981296	9.402451	12.502405
Ni	1.992345	6.856003	12.646469
Ni	4.796364	6.678547	11.191947
Ni	4.609696	7.005179	14.408084
Cl	1.019866	5.444611	10.977921
Cl	5.945549	7.848428	9.447388
Cl	3.539457	5.939015	16.245998
O	3.141552	7.986354	11.249226
O	2.972398	8.219313	13.923276
O	5.454973	7.955514	12.761889
O	3.814293	5.83942	12.8462
O	5.355818	10.331314	11.135912
H	5.603319	9.601585	10.493454
H	4.918404	11.013942	10.593468
O	1.270183	5.563586	14.218648
H	1.920356	5.654369	14.973601
H	0.417073	5.878448	14.570791
O	5.184333	8.67791	15.848389
H	4.593325	8.505172	16.608921
H	6.085524	8.564134	16.207626
O	3.778725	5.50788	9.697542
H	2.817181	5.482442	9.981617
H	3.806115	6.050372	8.886489
N	-0.36691	9.649906	14.489961
N	0.446139	8.136853	13.051122
N	8.66876	6.703083	14.029333
N	6.528653	6.339943	14.580821
C	1.988343	9.957803	10.608392
N	1.09036	10.760247	9.969506
C	1.000918	11.93897	10.704515
C	0.250954	13.101661	10.510206
H	-0.422605	13.218502	9.660908
C	0.408104	14.114231	11.459412
H	-0.156586	15.040787	11.347065
C	1.281577	13.967422	12.557708
H	1.375046	14.785108	13.273913
C	2.028786	12.804029	12.747891
H	2.707219	12.691709	13.593973
C	1.882134	11.780026	11.803729
N	2.47972	10.528381	11.709785

C	2.456387	8.598853	10.170554
H	1.603351	7.973472	9.852365
H	3.131326	8.709274	9.29914
C	0.385728	10.480911	8.723334
H	0.769847	11.121192	7.917927
H	-0.687458	10.667621	8.854682
H	0.534378	9.432158	8.448763
C	0.706719	8.897379	14.115052
C	-1.401654	9.348789	13.609729
C	-2.71693	9.813566	13.52955
H	-3.114189	10.544521	14.234334
C	-3.503557	9.29179	12.500234
H	-4.537521	9.624788	12.399685
C	-2.991671	8.342946	11.589966
H	-3.641788	7.960672	10.80142
C	-1.677359	7.881104	11.674658
H	-1.278865	7.14292	10.978255
C	-0.876002	8.394036	12.702773
C	2.046354	8.848238	14.792319
H	2.380775	9.866158	15.058407
H	1.958112	8.275209	15.736072
C	-0.457738	10.558527	15.627305
H	0.542528	10.735091	16.034388
H	-1.093352	10.125088	16.411192
H	-0.884827	11.515313	15.302226
C	5.343947	4.131485	12.251127
N	6.017237	2.945525	12.299542
C	7.163591	3.097488	11.525881
C	8.20199	2.214328	11.219313
H	8.221155	1.192629	11.599758
C	9.218224	2.703995	10.395446
H	10.048471	2.04885	10.127783
C	9.193124	4.024755	9.899346
H	10.006131	4.364914	9.255998
C	8.153799	4.903541	10.20906
H	8.124731	5.921971	9.820603
C	7.126966	4.427358	11.034355
N	5.976633	5.042045	11.512428
C	4.01968	4.437963	12.891341
H	3.212712	3.918759	12.339676
H	3.993012	4.073125	13.933323
C	5.608256	1.723261	12.981525
H	4.770594	1.941605	13.651024
H	6.44513	1.333155	13.574172
H	5.296385	0.964401	12.251151
C	7.367368	7.052041	13.826358
C	8.675238	5.695947	14.990146
C	9.721373	4.980328	15.578152
H	10.763669	5.161349	15.314317
C	9.366421	4.018815	16.526815

H	10.150403	3.436433	17.012867
C	8.018295	3.785569	16.871824
H	7.786441	3.026022	17.620008
C	6.976746	4.503465	16.282236
H	5.934135	4.332735	16.55103
C	7.317082	5.472128	15.329629
C	6.854716	8.123384	12.90689
H	7.092919	9.116	13.333875
H	7.353226	8.068611	11.923156
C	9.84956	7.295308	13.410813
H	10.508233	6.500967	13.038552
H	10.395481	7.907567	14.141185
H	9.543907	7.926642	12.570797
O	4.654601	10.692899	14.03854
H	5.432371	11.218922	13.775747
H	4.949132	10.116553	14.791802

Structure upon one-electron oxidation

Ni	3.990391	9.393122	12.531487
Ni	1.926522	6.862144	12.725077
Ni	4.68282	6.634212	11.221016
Ni	4.617665	7.000507	14.443746
Cl	0.905208	5.510275	11.07753
Cl	5.777186	7.670554	9.553135
Cl	3.552417	5.875507	16.206956
O	3.198551	7.940552	11.278535
O	2.975823	8.201077	13.946519
O	5.442819	7.926352	12.789363
O	3.75024	5.859731	12.759538
O	5.37914	10.306798	11.186521
H	5.621625	9.602038	10.53011
H	4.989129	11.028719	10.65801
O	1.272104	5.583774	14.244847
H	1.900138	5.666947	15.023257
H	0.387586	5.82101	14.581205
O	5.209127	8.612213	15.829127
H	4.658028	8.505999	16.631288
H	6.125897	8.505728	16.152083
O	3.624719	5.406418	9.792059
H	2.652816	5.425624	10.046512
H	3.68683	5.809966	8.905137
N	-0.312362	9.715953	14.530593
N	0.458154	8.168709	13.111194
N	8.654635	6.618712	14.001506
N	6.513632	6.275323	14.559833
C	2.043135	9.877166	10.573727
N	1.139491	10.650582	9.913918
C	1.001095	11.827771	10.645816
C	0.222856	12.967967	10.430591
H	-0.436711	13.061526	9.567832

C	0.333039	13.986833	11.378622
H	-0.255458	14.896364	11.2517
C	1.187971	13.869536	12.495376
H	1.243602	14.692432	13.209234
C	1.963606	12.729354	12.706284
H	2.628144	12.638999	13.565632
C	1.862521	11.699167	11.76298
N	2.496226	10.463761	11.684399
C	2.545362	8.527924	10.147372
H	1.72202	7.876959	9.811153
H	3.260863	8.639702	9.312941
C	0.46096	10.350457	8.656811
H	0.771299	11.066696	7.885007
H	-0.625462	10.41307	8.797228
H	0.722929	9.339369	8.331323
C	0.738231	8.933853	14.170692
C	-1.350889	9.437987	13.645391
C	-2.649751	9.944823	13.558423
H	-3.023073	10.694264	14.256401
C	-3.450214	9.441096	12.531959
H	-4.472223	9.806982	12.425684
C	-2.966762	8.469514	11.630538
H	-3.626192	8.102773	10.842627
C	-1.669385	7.964523	11.721498
H	-1.296493	7.20998	11.029311
C	-0.854833	8.459101	12.74807
C	2.076233	8.846967	14.841145
H	2.445705	9.849091	15.113696
H	1.985936	8.260944	15.775076
C	-0.381386	10.648028	15.651661
H	0.596707	10.707957	16.137921
H	-1.123707	10.300069	16.381552
H	-0.664921	11.644148	15.289428
C	5.265364	4.167023	12.221504
N	6.017814	3.046268	12.29192
C	7.174785	3.2814	11.551768
C	8.276661	2.463856	11.290309
H	8.343561	1.450701	11.686474
C	9.287459	3.007292	10.49825
H	10.165967	2.403725	10.267888
C	9.197278	4.319799	9.990042
H	10.009492	4.707731	9.374093
C	8.096669	5.135108	10.251768
H	8.024967	6.1451	9.851909
C	7.072163	4.601826	11.043495
N	5.85956	5.121095	11.488264
C	3.920797	4.43312	12.807933
H	3.12959	3.939906	12.217385
H	3.840908	4.090682	13.851748
C	5.6907	1.806135	12.990834

H	4.77123	1.945492	13.567018
H	6.508498	1.541243	13.671935
H	5.541977	0.998199	12.263162
C	7.359916	6.987058	13.810194
C	8.651739	5.596253	14.947267
C	9.692597	4.857445	15.515773
H	10.734901	5.027907	15.245641
C	9.330344	3.886905	16.451446
H	10.109011	3.285543	16.922354
C	7.98134	3.666296	16.802389
H	7.74471	2.898202	17.540067
C	6.945326	4.406524	16.232275
H	5.902663	4.24339	16.504417
C	7.293767	5.385159	15.293018
C	6.851336	8.077561	12.912781
H	7.093357	9.064433	13.348228
H	7.33343	8.039421	11.921227
C	9.841839	7.198096	13.381293
H	10.446396	6.403648	12.926645
H	10.440214	7.724824	14.136153
H	9.539399	7.907949	12.605516
O	4.637447	10.667249	14.042052
H	5.377896	11.246035	13.779803
H	4.970054	10.115809	14.795989

Structure upon deprotonation

Ni	4.007575	9.332569	12.39446
Ni	1.955245	6.841088	12.595786
Ni	4.793909	6.579156	11.144030
Ni	4.566713	6.985626	14.380811
Cl	0.992325	5.512629	10.890951
Cl	5.962967	7.624462	9.355613
Cl	3.494909	5.847409	16.166411
O	3.204752	8.011838	11.203870
O	2.935917	8.178009	13.857159
O	5.372965	7.963099	12.705265
O	3.777712	5.816215	12.802091
O	5.371348	10.181620	10.875409
H	5.580437	9.436096	10.239479
H	4.948716	10.875792	10.335927
O	1.224797	5.565637	14.130001
H	1.869592	5.633733	14.893051
H	0.367718	5.869157	14.483480
O	5.047198	8.578037	15.848108
H	4.483073	8.311642	16.602950
H	5.959638	8.489134	16.185237
O	3.773827	5.398957	9.719252
H	2.796669	5.422339	9.949071
H	3.868402	5.858097	8.862410
N	-0.379372	9.663902	14.421166

N	0.430445	8.160208	12.970820
N	8.631606	6.876482	13.963183
N	6.512877	6.408039	14.517637
C	2.041149	9.952883	10.603232
N	1.118157	10.792044	10.074828
C	1.073031	11.920604	10.892871
C	0.309171	13.087551	10.813300
H	-0.412055	13.248983	10.012017
C	0.515868	14.040804	11.811403
H	-0.058168	14.967871	11.787679
C	1.451476	13.834303	12.847037
H	1.582939	14.608435	13.604238
C	2.213796	12.668909	12.926159
H	2.944976	12.504705	13.716157
C	2.013982	11.704009	11.931691
N	2.595066	10.461256	11.712118
C	2.519123	8.627088	10.107756
H	1.690584	7.977257	9.781158
H	3.207627	8.763802	9.253610
C	0.331585	10.585750	8.862085
H	0.600142	11.340453	8.111894
H	-0.737611	10.664302	9.095067
H	0.541073	9.589938	8.461038
C	0.692463	8.916018	14.038885
C	-1.415515	9.369924	13.539461
C	-2.729275	9.839693	13.464077
H	-3.122886	10.567408	14.174028
C	-3.518367	9.327416	12.432279
H	-4.551210	9.664524	12.334708
C	-3.009938	8.384212	11.514335
H	-3.661600	8.010179	10.723225
C	-1.697259	7.917141	11.594129
H	-1.302503	7.185109	10.889376
C	-0.893415	8.420071	12.625444
C	2.035836	8.869850	14.706325
H	2.406383	9.888613	14.914518
H	1.951670	8.342791	15.676071
C	-0.463051	10.576768	15.556189
H	0.517004	10.652299	16.036671
H	-1.192227	10.202056	16.286437
H	-0.771451	11.572355	15.212610
C	5.303645	4.080297	12.299296
N	5.980209	2.902857	12.411250
C	7.153588	3.036728	11.674737
C	8.206359	2.149553	11.437627
H	8.216428	1.142406	11.854960
C	9.249470	2.615815	10.634548
H	10.091926	1.956467	10.420988
C	9.236482	3.918194	10.091656
H	10.070474	4.240294	9.466208

C	8.183118	4.801600	10.332348
H	8.164224	5.805376	9.907297
C	7.129509	4.348158	11.136171
N	5.958595	4.969757	11.552924
C	3.958234	4.408686	12.878053
H	3.169081	3.893032	12.299564
H	3.878892	4.065962	13.923983
C	5.555079	1.700930	13.119843
H	4.666254	1.924311	13.717710
H	6.357620	1.360240	13.786035
H	5.313923	0.904080	12.403607
C	7.316335	7.175599	13.777766
C	8.686179	5.845319	14.897072
C	9.765548	5.160505	15.461172
H	10.797442	5.390710	15.195129
C	9.456618	4.162615	16.387770
H	10.267223	3.601337	16.854461
C	8.121649	3.864822	16.735545
H	7.927288	3.078713	17.466701
C	7.047051	4.551993	16.169922
H	6.014212	4.330845	16.439832
C	7.341844	5.555907	15.239190
C	6.760446	8.242925	12.880057
H	6.888982	9.240574	13.336776
H	7.271404	8.250535	11.903261
C	9.785216	7.524453	13.348574
H	10.428738	6.768440	12.881355
H	10.358924	8.071707	14.108196
H	9.445905	8.228289	12.582392
O	4.667350	10.531611	13.628226
H	4.776540	10.001084	14.447679

References

- [1] S. K. Poddar, N. Saqueeb, *J. Pharm. Sci.* **2016**, 15, 83.
- [2] S. Stoll and A. Schweiger, *J. Magn. Reson.* **2006**, 178, 42.
- [3] F. Neese, *Wiley Interdiscip. Rev. Comput. Mol. Sci.* **2012**, 2, 73.
- [4] J. P. Perdew, *Phys. Rev. B* **1986**, 33, 8822.
- [5] J. P. Perdew, *Phys. Rev. B* **1986**, 34, 7406.
- [6] A. D. Becke, *Phys. Rev. A* **1988**, 38, 3098.
- [7] A. Schäfer, C. Huber, R. J. Ahlrichs, *Chem. Phys.* **1994**, 100, 5829.
- [8] F. Neese, *J. Comput. Chem.* **2003**, 24, 1740.
- [9] F. Weigend, *Phys. Chem. Chem. Phys.* **2006**, 8, 1057.
- [10] V. Barone, M. Cossi, *J. Phys. Chem. A*, **1998**, 102, 1995.
- [11] A. D. Becke, *J. Chem. Phys.* **1993**, 98, 1372.
- [12] C. T. Lee, W. T. Yang, R. G. Parr, *Phys. Rev. B* **1988**, 37, 785.
- [13] L. Noodleman *J. Chem. Phys.* **1981**, 74, 5737.
- [14] L. Noodleman, D. A. Case, *Adv. Inorg. Chem.* **1992**, 38, 423.
- [15] L. Noodleman, E. R. Davidson, *Chem. Phys.* **1986**, 109, 131.
- [16] J. Ho, *Phys. Chem. Chem. Phys.*, **2015**, 17, 2859.
- [17] L. Yan, Y. Lu, *Phys. Chem. Chem. Phys.* **2016**, 18, 5529.
- [18] F. Neese, *Inorg. Chim. Acta* **2002**, 337, 181.

- [19] V. Barone, In *Recent Advances in Density Functional Methods*, **1996**; Chong, D. P., Ed.; World Scientific: Singapore, Part I.
- [20] J. P. Perdew, K. Burke, M. Ernzerhof. *J. Chem. Phys.* **1996**, 105, 9982.
- [21] a) M. E. Casida, In *Recent Advances in Density Functional Theory*; **1995**; Chong, D. P., Ed.; World Scientific: Singapore, Part I; b) R. E. Stratmann, G. E. Scuseria, M. J. Frisch. *J. Chem. Phys.* **1998**, 109, 8218; c) R. Bauernschmitt, R. Ahlrichs. *Chem. Phys. Lett.* **1996**, 256, 454; d) S. Grimme. *J. Chem. Phys.*, **2013**, 138, 244104; e) C. Bannwarth, S. Grimme. *Comp. Theor. Chem.* **2014**, 1040–1041, 45.
- [22] a) S. Hirata, M. Head-Gordon. *Chem. Phys. Lett.* **1999**, 314, 29; b) S. Hirata, M. Head-Gordon. *Chem. Phys. Lett.* **1999**, 302, 375.
- [23], F. Neese. *J. Chem. Phys.* **2001**, 115, 11080.
- [24] Chemcraft, <http://chemcraftprog.com>
- [25] J. Zhang, V. Frankevich, R. Knochenmuss, S. D. Friess, R. Zenobi. *J. Am. Soc. Mass. Spectrom.* **2003**, 14, 42–50.
- [26] J. Janisch, A. Ruff, B. Speiser, C. Wolff, J. Zigelli, S. Benthin, V. Feldmann, H. A. Mayer. *J. Solid State Electrochem.* **2011**, 15, 2083.
- [27] M. L. Pegis, J. A. S. Roberts. *Inorg. Chem.* **2015**, 54, 11883.
- [28] A. M. Appel and M. L. Helm. *ACS Catal.* **2014**, 4, 630.
- [29] a) L.-H. Zhang, F. Yu, Y. Shi, F. Li, H. Li, *Chem. Commun.* **2019**, 55, 6122. b) A. G. Walden, A. J. M. Miller, *Chem. Sci.* **2015**, 6, 2405. c) E. S. Rountree, B. D. McCarthy, T. T. Eisenhart, J. L. Dempsey, *Inorg. Chem.* **2014**, 53, 9983.
- [30] Wei-Song Gao, Jin-Miao Wang, Ning-Ning Shi, Chang-Neng Chen, Yu-Hua Fan and Mei Wang. *New J. Chem.* **2019**, 43, 4640.
- [31] *Electrochemical Methods: Fundamentals and Applications*, 2nd Ed.; Wiley: New York, **2000**.